

การดูฉบับของมีเทนในเมทัลลอร์แกนิกเฟรมเวิร์กศึกษาโดยการคำนวณทางเคมีควอนตัม



นางสาว รัชฎยา ศีลภูษิต

สถาบันวิทยบริการ
จุฬาลงกรณ์มหาวิทยาลัย

วิทยานิพนธ์นี้เป็นส่วนหนึ่งของการศึกษาตามหลักสูตรปริญญาวิทยาศาสตรมหาบัณฑิต

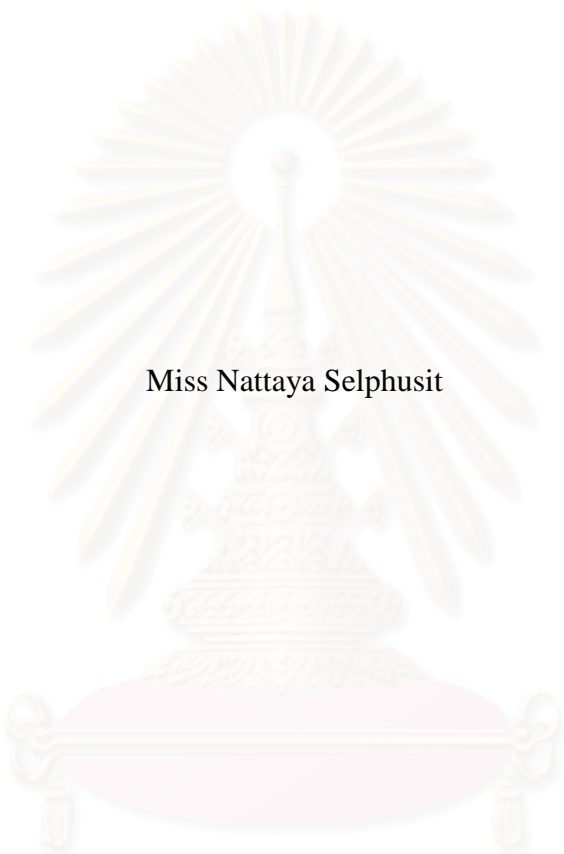
สาขาวิชาปิโตรเคมีและวิทยาศาสตร์พอลิเมอร์

คณะวิทยาศาสตร์ จุฬาลงกรณ์มหาวิทยาลัย

ปีการศึกษา 2550

ลิขสิทธิ์ของจุฬาลงกรณ์มหาวิทยาลัย

ADSORPTION OF METHANE IN METAL ORGANIC FRAMEWORK AS
STUDIED BY QUANTUM CHEMICAL CALCULATIONS



Miss Nattaya Selphusit

สถาบันวิทยบริการ

จุฬาลงกรณ์มหาวิทยาลัย

A Thesis Submitted in Partial Fulfillment of the Requirements
for the Degree of Master of Science Program in Petrochemistry and Polymer Science

Faculty of Science

Chulalongkorn University

Academic Year 2007

Copyright of Chulalongkorn University

Thesis Title ADSORPTION OF METHANE IN METAL ORGANIC
FRAMEWORK AS STUDIED BY QUANTUM CHEMICAL
CALCULATIONS

By Miss Nattaya Selphusit

Field of Study Petrochemistry and Polymer Science

Thesis Advisor Anawat Ajavakom, Ph. D.

Thesis Co-advisor Professor Supot Hannongbua, Ph. D.

Accepted by the Faculty of Science, Chulalongkorn University in Partial
Fulfillment of the Requirements for the Master's Degree

S. Hannongbua
..... Dean of the Faculty of Science
(Professor Supot Hannongbua, Ph. D.)

THESIS COMMITTEE

Sup Tan
..... Chairman
(Associate Professor Supawan Tantayanon, Ph. D.)

Anawat Ajavakom
..... Thesis Advisor
(Anawat Ajavakom, Ph. D.)

S. Hannongbua
..... Thesis Co-advisor
(Professor Supot Hannongbua, Ph. D.)

Warinthorn Chavasiri
..... Member
(Assistant Professor Warinthorn Chavasiri, Ph. D.)

Duangamol Nuntasri
..... Member
(Duangamol Nuntasri, Ph. D.)

ฉันทยา ศิลฎญิต : การดูดซับของมีเทนในเมทัลลอร์แกนิกเฟรมเวิร์กศึกษาโดยการคำนวณทางเคมีควอนตัม. (ADSORPTION OF METHANE IN METAL ORGANIC FRAMEWORK AS STUDIED BY QUANTUM CHEMICAL CALCULATIONS)

อ.ที่ปรึกษา: อ.ดร. อนวัช อาชวคม, อ.ที่ปรึกษาร่วม: ศ. ดร. สุพจน์ หารหนองบัว, 71 หน้า.

งานวิจัยนี้ได้ศึกษาดำเนินการดูดซับและพลังงานการยึดจับของมีเทนในพื้นที่ผิวของเมทัลลอร์แกนิกเฟรมเวิร์ก (IRMOF) 3 ชนิด ได้แก่ IRMOF-1, IRMOF-6 และ IRMOF-14 โดยโครงสร้างที่ดีที่สุดของ IRMOF ได้จากการคำนวณโดยวิธี DFT(B3LYP/6-31G**) ทั้งนี้โครงสร้างของ IRMOF ทั้งสามชนิดได้ถูกแทนด้วย คลัสเตอร์ 3 แบบ คือ แบบเดี่ยว แบบคู่ และแบบสาม ส่วนโครงสร้างการจัดเรียงตัวของมีเทนที่ใช้ทำการศึกษา มี 2 ลักษณะ คือ ไฮโดรเจนหนึ่งอะตอมของมีเทนที่เข้าและออกจากลิงก์เกอร์ และมุมของเมทัลลอร์แกนิกเฟรมเวิร์กชนิดต่างๆ ผลการศึกษาพบว่าระดับทฤษฎีทางกลศาสตร์ควอนตัม ONIOM(MP2/6-31G** : HF/6-31G**) ที่รวมการแก้ไขความคลาดเคลื่อนเนื่องจากการซ้อนทับของเบสิสเซต (BSSE) เป็นวิธีที่เหมาะสมสำหรับระบบที่ศึกษา และยังพบว่าพบว่าคลัสเตอร์แบบเดี่ยวมีขนาดใหญ่เพียงพอที่จะใช้แทน IRMOF ได้ การดูดซับที่ดีที่สุดของโมเลกุลมีเทน IRMOF-1 และ IRMOF-6 เป็น -3.64 และ -3.53 กิโลจูลต่อโมล ซึ่งการดูดซับเกิดขึ้นที่มุมมีโครงสร้างของมีเทนแบบไฮโดรเจนหนึ่งอะตอมที่ออก ส่วนใน IRMOF-14 ค่าการดูดซับเท่ากับ -3.77 กิโลจูลต่อโมล เกิดขึ้นที่ลิงก์เกอร์โดยโครงสร้างของมีเทนเป็นแบบที่ไฮโดรเจนหนึ่งอะตอมที่เข้า

สาขาวิชา..ปิโตรเคมีและวิทยาศาสตร์พอลิเมอร์.....ลายมือชื่อนิสิตฉันทยา ศิลฎญิต
ปีการศึกษา2550.....ลายมือชื่ออาจารย์ที่ปรึกษา
ลายมือชื่ออาจารย์ที่ปรึกษาร่วม.....

4872284623 : MAJOR PETROCHEMISTRY AND POLYMER SCIENCE

KEY WORD: METAL ORGANIC FRAMEWORK/IRMOFs/MOF-5/IRMOF-1/
IRMOF-6/IRMOF-14/METHANE/ONIOM/
QUANTUM CALCULATION

NATTATA SELPHUSIT: ADSORPTION OF METHANE IN METAL
ORGANIC FRAMEWORK AS STUDIED BY QUANTUM CHEMICAL
CALCULATIONS. THESIS ADVISOR: ANAWAT AJAVAKOM, Ph.D.
THESIS CO-ADVISOR: PROF. SUPOT HANNONGBUA, Ph. D., 71 pp.

Optimal binding sites and the corresponding binding energies between CH₄ molecules and three type of IRMOF namely IRMOF-1, IRMOF-6 and IRMOF-14. The IRMOF structures were optimized using the DFT calculation with the 6-31G** basis set. The clusters were validated using three different sizes of IRMOF clusters, SINGLE, DOUBLE and TRIPLE. CH₄ molecules were assigned to approach the linker (LINK) and corner (CORN) domains of the clusters in the H-in and H-out configurations. The ONIOM(MP2/6-31G**:HF/6-31G**) with the corrections due to the basis set superposition errors was found to be the optimal choice for the investigated systems. Among the three cluster sized, SINGLE cluster is sufficient to represent interactions with CH₄. The optimal binding sites of CH₄ molecules as well as their orientations in the cavity of the IRMOFs are CORN (H-out) for IRMOF-1 and IRMOF-6 with the corresponding binding energies of -3.64 and -3.53 kJ/mol, respectively. The corresponding binding energies for IRMOF-14 is -3.77 kJ/mol in the H-in configuration at LINK domain.

Field of study...Petrochemistry and Polymer Science...Student's signature...*Nattaya*...

Academic year.....2007.....Advisor's signature...*A. Javakom*...

Co-advisor's signature...*S. Hannongbua*...

ACKNOWLEDGMENTS

I would like to express my deep gratitude to people who give me the guidance, help and support to accomplish my study. First of all, I would like to give all affectionate gratitude to my beloved parents for all their love, support and encouragement during the whole period of my study. In particular, from their understanding and make me strong to overcome any obstacle.

I am truly grateful to Dr. Anawat Ajavakom, my advisor, for his multifarious understanding, useful guidance, kind suggestions and encouragement throughout this study. Gratefully thanks to Prof. Dr. Supot Hannongbua, my co-advisor, for good advice. I also would like to thank Dr. Tawun Remsungnen, Dr. Arthorn Loisuangsin, Dr. Atchara Pianwanitc, Dr. Oraphan Saengsawang, Mr. Rungroj Chanajaree and Mr. Arthit Vongachariya for kind suggestions and discussions.

I would like to specially thank thesis committees Assoc. Prof. Dr. Supawan Tantayanon, Assist. Prof. Dr. Warinthorn Chavasiri and Dr. Duangamol Nuntasri.

Finally, I would like to acknowledge the Computational Chemistry Unit Cell (CCUC) and Computer Center for Advance Research at Faculty of Science, Chulalongkorn University for computer resources and other facilities. I am also grateful to the Thailand Research Fund (TRF) and the National Research Council of Thailand (NRCT) for financial support during the study.

สถาบันวิทยบริการ
จุฬาลงกรณ์มหาวิทยาลัย

CONTENTS

	Page
ABSTRACT IN THAI	iv
ABSTRACT IN ENGLISH	v
ACKNOWLEDGEMENTS	vi
CONTENTS	vii
LIST OF TABLES	x
LIST OF FIGURES	xi
LIST OF ABBREVIATIONS	xiv
CHAPTER I INTRODUCTION	1
1.1 Research Rationale.....	1
1.2 Energy Resource.....	1
1.2.1 Hydrocarbon.....	1
1.2.2 Petroleum	2
1.2.3 Natural Gas.....	2
1.3 Metal Organic Frameworks (MOFs).....	3
1.3.1 What a MOFs is.....	4
1.3.2 Classification of MOFs	5
1.3.3 Synthesis of MOFs.....	7
1.3.4 Properties of MOFs.....	8
a) Porosity of MOFs.....	8
b) Gas Sorption of MOFs.....	9
1.3.5 Application.....	10
1.4 Adsorption.....	10
1.4.1 Physisorption.....	11
1.4.2 Chemisorption.....	11
1.5 Literature Reviews.....	11
1.6 Scope of This Study.....	13

CHAPTER II THEORETICAL BACKGROUND	14
2.1 Quantum Chemistry.....	14
2.2 Computational Chemistry.....	15
2.3 <i>Ab initio</i> Method.....	16
2.3.1 Hartree-Fock Method.....	16
2.3.2 Møller-Plesset Perturbation Theory.....	18
2.4 Density Functional Theory Methods.....	18
2.5 Semi-empirical Methods.....	19
2.5.1 AM1 Method.....	19
2.5.2 PM3 Method.....	20
2.6 Basis Set.....	20
2.6.1 Minimal Basis Sets.....	20
2.6.2 Split-valence basis sets.....	21
2.6.3 Polarization Functions.....	21
2.6.4 Diffuse Functions.....	21
2.7 Basis Set Superposition Error.....	22
2.8 ONIOM Method.....	22
2.9 GAUSSIAN Program.....	23
CHAPTER III CALCULATION DETAILS	24
3.1 Interaction Between Methane Molecule and Aromatic Systems.....	24
3.2 Initial Structure of IRMOFs Lattice.....	26
3.2.1 IRMOF-1.....	26
3.2.2 IRMOF-6.....	30
3.2.3 IRMOF-14.....	33

CHAPTER IV RESULTS AND DISCUSSION	35
4.1 Interaction Between Methane Molecule and Aromatic Systems.....	35
4.2 Geometries of the IRMOF-1.....	39
4.3 Interaction of CH ₄ in IRMOF-1 and Effect of BSSE	41
4.4 Binding Energy of CH ₄ in IRMOF-6 and IRMOF-14	50
CHAPTER V CONCLUSION	55
REFERENCES	56
APPENDICES	63
VITAE	71

สถาบันวิทยบริการ
จุฬาลงกรณ์มหาวิทยาลัย

LIST OF TABLES

Table		Page
4.1	The binding energies (kJ/mol) with the BSSE corrections of the optimized CH ₄ -C ₆ H ₆ complex and its derivatives CH ₄ -C ₆ H ₅ X (X = F, CN, OH, NH ₂ and CH ₃).....	36
4.2	The bond distances and bond angles obtained from the geometry optimizations as shown in Figure 3.2a.....	40
4.3	ONIOM binding energies with and without BSSE corrections and the corresponding distances between IRMOF-1 linker in the three cluster models (SINGLE, DOUBLE and TRIPLE) and CH ₄ molecule.....	41
4.4	ONIOM binding energies with and without BSSE corrections and the corresponding distances between IRMOF-1 corner in the three cluster models (SINGLE, DOUBLE and TRIPLE) and CH ₄ molecule.....	42
4.5	ONIOM binding energies with BSSE corrections and the corresponding distances between IRMOF-6 linker in the three cluster models (SINGLE, DOUBLE and TRIPLE) and CH ₄ molecule.....	41
4.6	ONIOM binding energies with BSSE corrections and the corresponding distances between IRMOF-6 corner in the three cluster models (SINGLE, DOUBLE and TRIPLE) and CH ₄ molecule.....	52
4.7	ONIOM binding energies and the corresponding distance with the BSSE corrections for the CH ₄ -IRMOF-14 complex.....	53

สถาบันวิทยบริการ
 จุฬาลงกรณ์มหาวิทยาลัย

LIST OF FIGURES

Figure	Page
1.1	Porous Metal-Organic particle-like structure.....4
1.2	A series of Isoreticular Metal–Organic Frameworks (IRMOFs).....5
1.3.	Carboxylate links in series of IRMOFs.....6
1.4	SBUs (a) the square “paddlewheel”, with two terminal ligand sites, (b) the octahedral “basic zinc acetate” cluster, and (c) the trigonal prismatic oxo-centered trimer, with three terminal ligand sites.....7
1.5	The porosity of MOFs compared to zeolites. Blue circles, sorption and crystal MOF structures; red squares, crystal MOF structures; yellow, diamonds, some typical zeolites. Reference numbers (superscripted) are shown in green.....9
2.1	Flow chart of the HF procedure17
3.1	Twelve different models to investigate for the binding energies between CH ₄ and benzene derivatives, (a),(g) benzene, (b),(h) aniline, (c),(i) cyanobenzene, (d),(j) fluorobenzene, (e),(k) phenol and (f),(l) xylene. Figures (a)-(f) are the H-in and Figures (g)-(l) are H-out, respectively.....25
3.2	(a) A single linker of the IRMOF-1 consisting of two corners and one linker and (b) The IRMOF-1 unit cell.....26
3.3	Models SINGLE, DOUBLE and TRIPLE represent the IRMOF-1 fragments containing one, two and three units as oriented, respectively.....27
3.4	Orientation of methane molecules in (a) H-in orientation and (b) H-out orientation to the binding site (linker or corner).....28
3.5	The real part (line) and the model part (ball and stick) for the ONIOM method of IRMOF-1, (a) at the linker and (b) at the corner.....29
3.6	(a) A single linker of the IRMOF-6 consisting of two corners and one linker (cyclobutylbenzene) and (b) The IRMOF-6 unit cell.....30
3.7	Models SINGLE, DOUBLE (Model I, II) and TRIPLE (Model I, II) represent the IRMOF-6 fragments containing one, two and three units as oriented, respectively.....31

Figure	Page
3.8	The real part (line) and the model part (ball and stick) for the ONIOM method of IRMOF-6, (a) at the linker and (b) at the corner.....32
3.9	(a) A single linker of the IRMOF-14 consisting of two corners and one linker (b) The IRMOF-14 unit cell.....33
3.10	Models SINGLE (Models I, II) and DOUBLE, TRIPLE (Models I, II,III) represent the IRMOF-14 fragments.....34
3.11	The real part (line) and the model part (ball and stick) for the ONIOM method of IRMOF-14, (a) at the linker and (b) at the corner.....34
4.1	Optimized structures of CH ₄ -C ₆ H ₆ (a, b) and CH ₄ -C ₆ H ₅ CN (c, d) with the starting configurations H-in (a, c) and H-out (b, d). The yellow (●), red (●) and green (●) balls are the carbon atoms obtained from the MP2, HF and B3LYP at the 6-31G** basis set, respectively.....35
4.2	The binding energies between CH ₄ and benzene derivatives at the optimal structures using MP2/6-31G**.....37
4.3	ONIOM binding energies (●) with BSSE and (■) without BSSE corrections for the CH ₄ /MOF-5 complexes where CH ₄ was located in the H-in configuration (a) for the SINGLE linker (LINK) and (b) for the SINGLE corner (CORN) calculations, the distances were measured from the C atom of CH ₄ to C _g and O ₁ , respectively (see Figure 3.2a).....43
4.4	ONIOM binding energies (●) with BSSE and (■) without BSSE corrections for the CH ₄ /MOF-5 complexes where CH ₄ was located in the H-in configuration (a) for the DOUBLE linker (LINK) and (b) for the DOUBLE corner (CORN) calculations, the distances were measured from the C atom of CH ₄ to C _g and O ₁ , respectively (see Figure 3.2a).....44
4.5	ONIOM binding energies (●) with BSSE and (■) without BSSE corrections for the CH ₄ /MOF-5 complexes where CH ₄ was located in the H-in configuration (a) for the TRIPLE linker (LINK) and (b) for the TRIPLE corner (CORN) calculations, the distances were measured from the C atom of CH ₄ to C _g and O ₁ , respectively (see Figure 3.2a).....45

Figure	Page
4.6 ONIOM binding energies (●) with BSSE and (■) without BSSE corrections for the CH ₄ /MOF-5 complexes where CH ₄ was located in the H-out configuration (a) for the SINGLE linker (LINK) and (b) for the SINGLE corner (CORN) calculations, the distances were measured from the C atom of CH ₄ to C _g and O ₁ , respectively (see Figure 3.2a).....	46
4.7 ONIOM binding energies (●) with BSSE and (■) without BSSE corrections for the CH ₄ /MOF-5 complexes where CH ₄ was located in the H-out configuration (a) for the DOUBLE linker (LINK) and (b) for the DOUBLE corner (CORN) calculations, the distances were measured from the C atom of CH ₄ to C _g and O ₁ , respectively (see Figure 3.2a).....	47
4.8 ONIOM binding energies (●) with BSSE and (■) without BSSE corrections for the CH ₄ /MOF-5 complexes where CH ₄ was located in the H-out configuration (a) for the DOUBLE linker (LINK) and (b) for the DOUBLE corner (CORN) calculations, the distances were measured from the C atom of CH ₄ to C _g and O ₁ , respectively (see Figure 3.2a).....	48

LIST OF ABBREVIATIONS

NG	=	Natural Gas
IRMOFs	=	Isorecticular Metal-Organic Frameworks
IRMOF-1	=	Isorecticular Metal-Organic Framework-1
IRMOF-6	=	Isorecticular Metal-Organic Framework-6
IRMOF-14	=	Isorecticular Metal-Organic Framework-14
MOFs	=	Metal-Organic Frameworks
CNG	=	Compressed Natural Gas
ANG	=	Adsorbed Natural Gas
SBU _s	=	Secondary Building Units
BDC	=	Benzenedicarboxylate
NDC	=	Naphthalenedicarboxylate
BPDC	=	Biphenyldicarboxylate
HPDC	=	Hydropyrenedicarboxylate
PDC	=	Pyrene 2,7-dicarboxylate
PDC	=	Pyrenedicarboxylate
TPDC	=	Terphenyldicarboxylate
XRD	=	X-ray Diffraction
3D	=	Threedimensional
DEF	=	Diethylformamide
HF	=	Hartree-Fock
N	=	Number
SCF	=	Self-Consistent Field
MP	=	Møller-Plesset Perturbation
DFT	=	Density Functional Theory
B3LYP	=	Becke's three parameter hybrid functional using the LYP correlation function

LIST OF ABBREVIATIONS

LYP	=	Lee-Yang-Parr functional
AM1	=	Austin Model 1
MNDO	=	Modified Neglect of Differential Overlap
PM3	=	Parameterized Model number 3
STO	=	Slater Type Orbital
STO-3G	=	Slater Type Orbital approximated by 3 GAUSSIAN type orbitals
BSSE	=	Basis Set Superposition Error
MO	=	Molecular Orbital
ONIOM	=	Our own N-layered Integrated molecular Orbital and Molecular mechanics
kJ/mol	=	Kilo Joule per mole
Å	=	Angström



สถาบันวิทยบริการ
จุฬาลงกรณ์มหาวิทยาลัย

CHAPTER I

INTRODUCTION

1.1 Research Rationale

Natural gas is a gaseous fuel primarily consisting of methane. The major difficulty in the use of natural gas is transportation and storage because of its low density. Therefore, an alternative approach is to seek for storage materials which provides energy security and easy for transportation. Various types such as carbon nanotube, carbon-based material zeolites and metal-organic framework (MOFs) are developed for methane storage. Among those materials, MOFs have become as a promising candidates for methane adsorption because of the following properties, *e.g.*, large pore sizes, high surface areas and selective uptake of small molecules. To develop and design new MOFs for methane storage, the interaction and orientation of methane molecule have been studied using computational calculation.

1.2 Energy Resource

1.2.1 Hydrocarbon

In organic chemistry, a hydrocarbon is an organic compound entirely consisting of hydrogen and carbon. With relation to chemical terminology, aromatic hydrocarbons or arenes, alkanes, alkenes and alkyne-based compounds composed only of carbon and hydrogen are referred to as "Pure" hydrocarbons, whereas other hydrocarbons with bonded compounds or impurities of sulphur or nitrogen, are referred to as "impure" hydrocarbons.

1.2.2 Petroleum

Liquid geologically-extracted hydrocarbons are referred to as petroleum (literally "rock oil") or mineral oil, while gaseous geologic hydrocarbons are referred to as natural gas. All are significant sources of fuel and raw materials as a feedstock for the production of organic chemicals and are commonly found in the Earth's subsurface using the tools of petroleum geology.

The extraction of liquid hydrocarbon fuel from a number of sedimentary basins has been integral to modern energy development. Hydrocarbons are mined from tar sands, oil shale and potentially extracted from sedimentary methane hydrates. These reserves require distillation and upgrading to produce synthetic crude and petroleum.

Oil reserves in sedimentary rocks are the principal source of hydrocarbons for the energy, transport and petrochemical industries. Hydrocarbons are of prime economic importance because they encompass the constituents of the major fossil fuels (coal, petroleum, natural gas, *etc.*) and plastics, paraffin, waxes, solvents and oils.

1.2.3 Natural Gas

Natural gas is a gaseous fossil fuel consisting primarily of methane. The major difficulty in the use of natural gas is transportation and storage because of its low density.

The natural gas is mainly stored in pressure vessels at 204 atm, which demands an expensive multistage compression. An alternative that reduces the costs and risks of that process is to store the natural gas as an adsorbed phase within a solid porous material, because the interactions of the gas molecules with the material allows a compression at lower pressures. Zeolites are typical examples of solid porous materials used for this application.

To develop a new MOFs material with methane storage. Methane adsorption mechanism into the porous MOFs has been studied by computational calculation. We propose in this work new porous materials with even higher capacity for natural gas storage called Isorecticular Metal-Organic Frameworks (IRMOFs)[1-4]. The IRMOFs consists of an isorecticular framework with a cubic lattice with tetrahedral Zn_4O clusters at the cube vertices and organic dicarboxylate aromatic linkers between the vertices. Therefore, each Zn_4O is connected to six linkers with an octahedral symmetry. IRMOFs are very versatile materials, since the organic linkers can be easily modified and functionalized.

1.3 Metal Organic Frameworks (MOFs)

The increasing demand for energy has led to an acceleration of efforts to utilize new technologies based on alternate sources such as hydrogen and natural gas. Natural gas, which consists mainly of methane, is widely available in many countries including Thailand. However, its application has been impeded by the absence of safety and economical techniques for storage compared as compressed natural gas (CNG). An attractive alternative to CNG is adsorbed natural gas (ANG), which is usually stored in carbon materials, zeolites, and other porous materials[1,5,6]. It has been suggested that these materials must incorporate some specific characteristics in their structure. Some of those are high surface area, low weight, accessible pores with diameters of a few angstroms, high interaction energies, fast kinetics for adsorption desorption, and full reversibility. Recently, a new family of hybrid inorganic-organic nanoporous materials[1,2], which belongs to the category of coordination polymer materials. These new materials are called Isorecticular Metal-Organic Frameworks (IRMOFs) or Metal-Organic Frameworks (MOFs).

1.3.1 What a MOF is

MOFs are hybrid materials where metal ions or small nano-clusters are linked into one-, two- or three-dimensional structures by multi-functional organic linkers forming into well defined structure. Nanoporous MOFs also have emerged recently as promising new candidates for adsorption and membrane separations. The self-assembly of metal ion, which act as coordination centers, linked together by a variety of polyatomic organic bridging ligands, can result in coordination polymers, easy approach chemical modification. However, the term coordination polymer is not very precise with regarding to the structural features of the material. MOFs are very interesting inorganic-organic hybrid materials with amazing high surfaces up to 4500 m² per gram because they exhibit high porosities and world record areas.

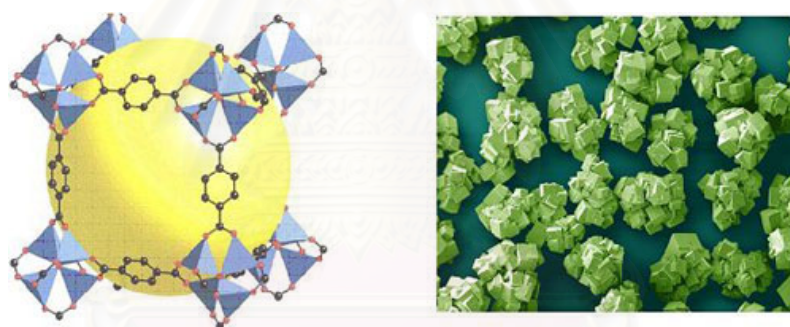


Figure 1.1 Porous Metal-Organic particle-like structure

The most prominent example of these MOF structures is MOF-5 (Figure 1.1), a metal-organic framework built from an extension of the basic zinc acetate structure (an octahedral $Zn_4O(CO_2)_6$ -benzenedicarboxylate).

1.3.2 Classification of MOFs

The series of MOFs (Figure 1.2) sharing the formula $Zn_4O(L)$ with L being a rigid linear dicarboxylate spacer demonstrates impressively the possibility in pore design given by a rational selection of the bridging entity. To produce materials with larger pores, 2,6-naphthalenedicarboxylate, 4,4'-biphenyldicarboxylate or 4,4-terphenyldicarboxylate were used for synthesis of MOF-5 with the replacement of 1,4-benzenedicarboxylate. All these materials exhibit the same cubic morphology as the prototypical MOF-5 with octahedral $Zn_4O(CO_2)_6$ clusters as secondary building unit (SBUs) link to organic linker (structures of the same net are formed) and the resulting structures are termed IRMOF-1 to IRMOF-16.

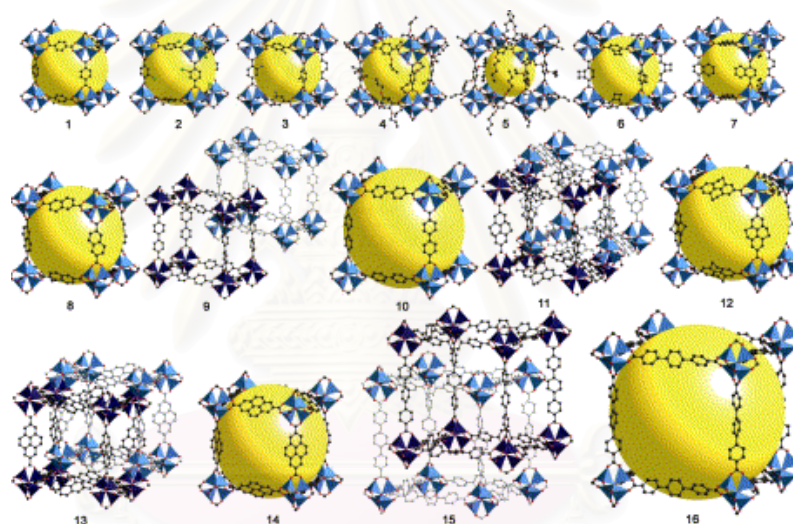


Figure 1.2 A series of Isoreticular Metal–Organic Frameworks (IRMOFs)

Indeed, using each of the links R2-BDC (Benzenedicarboxylate), R3-BDC, R4-BDC, R5-BDC, R6-BDC, R7-BDC, 2,6-NDC (Naphthalenedicarboxylate), BPDC (Biphenyldicarboxylate), HPDC (Hydropyrenedicarboxylate), PDC (Pyrenedicarboxylate), and TPDC (Terphenyldicarboxylate) instead of BDC yielded IRMOF-2 through -16, including the noninterpenetrating structures of BPDC, HPDC, PDC, and TPDC. Each member of the IRMOF series has been isolated and was formulated subsequently by chemical microanalysis and single-crystal XRD (X-ray Diffraction) studies.

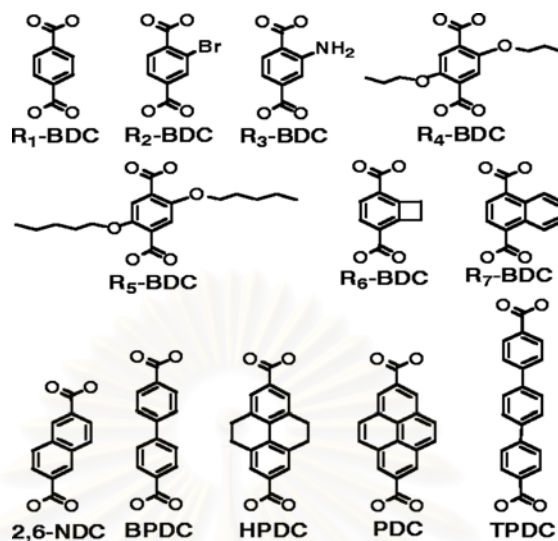


Figure 1.3 Carboxylate links in series of IRMOFs

All IRMOFs have the expected topology adapted by the prototype IRMOF-1 (Figure 1.3) in which an oxide-centered Zn_4O tetrahedron is edge-bridged by six carboxylates to give the octahedron-shaped secondary building unit that reticulates into a three-dimensional (3D) cubic porous network. However, the IRMOFs differ in the nature of functional groups decorating the pores and in the metrics of their pore structure.

สถาบันวิทยบริการ
จุฬาลงกรณ์มหาวิทยาลัย

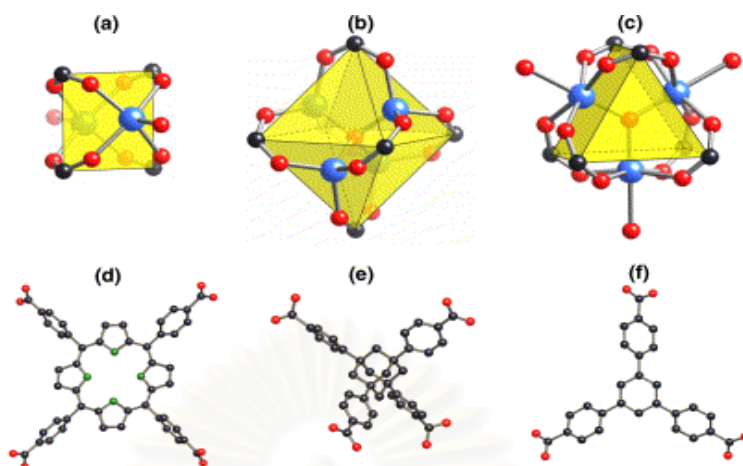


Figure 1.4 SBUs (a) the square “paddlewheel”, with two terminal ligand sites, (b) the octahedral “basic zinc acetate” cluster, and (c) the trigonal prismatic oxo-centered trimer, with three terminal ligand sites

Another metal carboxylate cluster that has been successfully used in the synthesis of porous networks is the bimetallic “paddlewheel”. This square SBU is generated *in situ* by the combination of four carboxylates with two metal cations such as Cu^{2+} , Zn^{2+} , Fe^{2+} , Mo^{2+} , Rh^{2+} , or $\text{Ru}^{2+, 3+}$, each capped by a labile solvent molecule (Figure 1.4). A variety of link geometries, such as linear, bent, trigonal, or tetrahedral have adjoined these clusters, often producing networks with simple and predictable topologies. Compounds in this class have provided nice examples of reticular synthetic principles, and have allowed the design of metal–organic backbones ranging from zero- to three-periodic. In all cases, these attributes were made possible by the use of appropriate links.

1.3.3 Synthesis of MOFs

These series of compounds exemplifies these attributes better than those sharing the formula $\text{Zn}_4\text{O}(\text{L})_3$, where L is a rigid linear dicarboxylate. These materials have the same cubic topology as prototypical MOF-5, In this context, the original low-yielding synthesis of MOF-5 was re-examined and developed into a high-yielding preparation: An *N,N'*-diethylformamide (DEF) solution mixture of $\text{Zn}(\text{NO}_3)_2 \cdot 4\text{H}_2\text{O}$

and the acid form of 1,4-benzenedicarboxylate (BDC) are heated (85° to 105°C) in a closed vessel to give crystalline MOF-5, $Zn_4O(R1-BDC)_3$ (where R1 = H), hereafter termed MOF-5, in 90% yield[7].

1.3.4 Properties of MOFs

MOFs have been found to have good properties for adsorption[7]. They have very high surface areas per unit volumes, and have very high porosities. Herein the important properties of MOFs are porosity and gas sorption will be described.

Porous media have potential applications in many fields, where confined species may alter the physical properties of the host material. MOFs materials have nanometer-sized channels with tailorable chemical functionality and are thus in principle attractive for the manipulation and transformation of a wide range of molecules.

a) Porosity of MOFs

In addition, demonstration of porosity through gas sorption isotherms is necessary to prove permanent porosity. Indeed, MOFs having structures based on inorganic SBUs are exceptionally porous with pore diameters and volumes which exceed those of the most porous and useful zeolite (Figure 1.5)[8-10]. Two important attributions of porous MOFs account for their structural stability and high porosity. In other porous solids such as zeolites and molecular sieves the interior of the pores is largely composed of walls leading to relatively lower specific capacity for sorption.

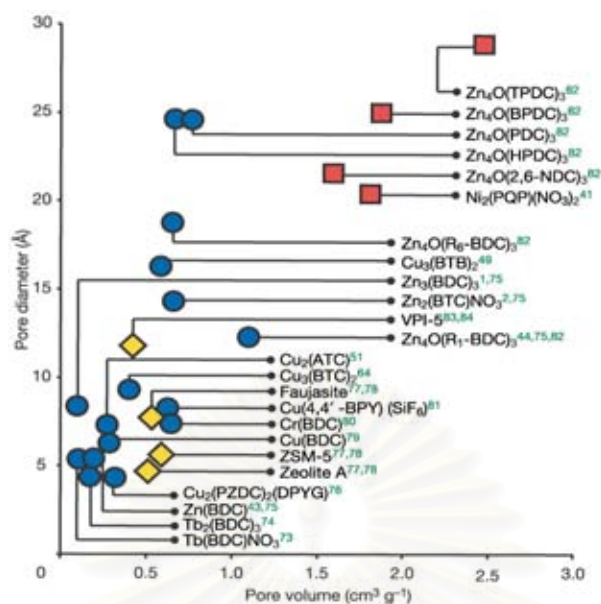


Figure 1.5 The porosity of MOFs compared to zeolites. Blue circles, sorption and crystal MOF structures; red squares, crystal MOF structures; yellow diamonds, some typical zeolites. Reference numbers (superscripted) are shown in green[4].

b) Gas Sorption of MOFs

Interestingly, the gas sorption properties of MOFs is now focused on increasing their uptake of fuel gases such as methane[1,11,12] and hydrogen[13]. The low carbon content and large chemical energies of these molecules make them highly attractive as replacements for fossil fuels. One of the obstacles to their widespread use is storage, especially for mobile applications. Host materials must satisfy a set of criteria including high gravimetric and volumetric uptake, facile gas release and reproducible cycling an economical production. Due to their large and reversible uptake of other gases, MOFs have been proposed as promising materials for this application. Reports have demonstrated that by changing the organic linkers in isorecticular materials, increases in their capacities for methane and hydrogen were actually realized[1,13].

1.3.5 Application

MOFs are crystalline porous solids composed of a three-dimensional (3D) network of metal ions held in place by multidentate organic molecules. The spatial organization of these structural units leads to a system of channels and cavities in the nanometer length scale, analogous to that found in zeolites. Correct selection of the structural subunits and the way in which they are connected allows systematic modification of the pore structure of MOFs. Over the last decade, the elevated surface area and pore volume and the flexibility of pore design characteristic of MOFs have sparked research aimed mainly at preparing new MOFs structures and studying their applications in separation[14,15], molecular storage[3,16,17], molecular magnets [18,19] and semiconductors[20].

Based on the similarity to zeolites, a logical application of MOFs could be as solid catalysts. However, despite the elevated metal content of MOFs, their use in catalysis is largely hampered by the relatively low stability to thermal treatments, chemical agents, and moisture, due to the presence of the organic component. Moreover, in most known MOFs structures, the co-ordination sphere of the metal ions is totally blocked by the organic linkers, so that the metal centers are not accessible to reactants. However, there are some precedents in the literature reporting some MOFs with accessible metal sites, opening the possibility of their use in catalysis. Consequently, despite the limited number of catalytic studies using MOFs as the active materials in catalysis and photocatalysis in the literature[21], their number can be anticipated to grow considerably in the near future.

1.4 Adsorption

Adsorption occurred on solid surface is a very important due to its wide potential application involved in the reaction with the surface of solid catalyst in the catalysis district. Generally, the investigations about the adsorption on solid surface can approximately be classified into two categories. One is the adsorption on the perfect surface, the other happens on the defective surface. It is normally agreed that the perfect surface, under most conditions, is chemically inert towards the adsorption and dissociation of small molecules and, in discrete contrast, the surface with various defect is able to display relatively high surface reactivity and thus contributes to the

catalytic reaction. Molecules and atoms can attach to surface of solid to two ways, physisorption (or physical adsorption) and chemisorption (or chemical adsorption).

1.4.1 Physisorption

Physisorption is mainly the result of Van der Waals interactions between the molecules of the adsorbing surface (the adsorbent) and the adsorbate molecules. Van der Waals interactions have a long range but are weak, and the energy released when a particle is physisorbed and often results in the formation of multilayers of adsorbate molecules. Physisorption usually is dominated at very low temperatures and occurs very rapidly.

1.4.2 Chemisorption

In chemisorption a bond is usually formed that is stronger than a Van der Waals bond. It need not be a covalent bond and tends to find sites that maximize their coordination number with adsorbate molecules. The enthalpy of chemisorption is greater than that for physisorption. A chemisorbed molecule may be torn apart at the demand of the surface atoms.

The enthalpy of adsorption depends on the extent of surface coverage, mainly because the adsorbate molecules interact. If the adsorbate molecules repel each other the enthalpy of adsorption becomes less exothermic as coverage increment. If the adsorbate molecules attract each other, then they tend to cluster together in island, and growth occurs at the borders.

1.5 Literature Reviews

The first MOFs, reported by Robson and others in the early 1990s, typically consisted of single metal ions connected by simple tetrahedral or rod-shaped ligands, such as tetracyanophenylmethane or 4,4' bipyridine[22-25], and had little or no practical applicability. The use of more varied organic linkers and the replacement of single metal ions with metal clusters however has been led to the synthesis of increasingly complex frameworks with a variety of proposed applications[26-28].

In 1984, Wells[29] gave the definition of structure predictability, an important requirement for the synthesis of functional materials with tailored properties, which has even become possible, in many cases by combining topological principles laid out.

In 1997, IRMOF materials were first synthesized by Yaghi and coworkers[30], as a first step, they concentrated on the material known as isorecticular metal-organic framework IRMOF-1. A new family of highly crystalline, porous materials in which the size and chemical functionality of the pores can be tailored systematically shows promise for gas-storage applications.

In 2000 Seo *et al.* addition, the organic part can be easily functionalized before the synthesis to yield different chemical environments within the IRMOFs cavities. As a result, these materials can also be used as new reaction media with controlled spatial, chiral and chemical properties[31].

In 2002, Eddaoudi *et al.* have shown that porous MOFs were successfully synthesized as to target the capability to store hydrogen and methane. They used the reticular approach to synthesize 16 different MOFs with the same underlying topology but different chemical functionality of the pores[1], functionalizing the pores allows for different hydrogen and methane storage capabilities was investigated. A similar concept was applied to target the electronic properties of these materials. In the same year, Eddaoudi studied methane adsorption by MOF-5 and the similar IRMOF-6. They showed that these new materials are superior for methane storage compared to current alternatives at room temperature[1].

In 2003, Rosi *et al.*[32] prepared MOFs in high yield and with adjustable pore size, shape, and functionality has led to their study as gas sorption materials and interesting properties, MOFs have been explored for various applications including the efficient storage of volatile fuels like hydrogen. Recently, Yaghi and co-workers reported that a series of IRMOFs, $Zn_4O(L)$ (L = linear aromatic dicarboxylates), have reversible hydrogen storage capacities.

In 2004, Sagara *et al.*[33] reported the results of quantum chemical calculations on H_2 binding by the MOF-5. Second-order Møller-Plesset perturbation theory was used to calculate the binding energy of H_2 to benzene and H_2 -1,4-benzenedicarboxylate- H_2 . The binding energy results were 4.77 kJ/mol for benzene, 5.27 kJ/mol for H_2 -1,4-benzenedicarboxylate- H_2 .

In 2005 Bordiga *et al.*[34] studied the physisorption on high surface area MOF-5, *ab initio* calculations showed that the adsorptive properties of this material are mainly due to dispersive interactions with the internal wall structure and to weak electrostatic forces associated with $O_{13}Zn_4$ clusters. Calculated and measured binding enthalpies were between 2.26 and 3.5 kJ/mol, in agreement with the H_2 rotational barriers reported in the literature. A minority of binding sites with higher adsorption enthalpy (7.4 kJ/mol) was also observed. These species are probably associated with OH groups on the external surfaces present as termini of the microcrystals.

In 2006 Coneliu Buda and Barry Dunitz[35] investigated physisorption of hydrogen on conjugated systems using *ab initio* methods. The best adsorption sites were related to the organic linker with special attention to the edge site, which was only recently reported to exist as the weakest adsorbing site in MOFs. The investigate of chemically modified models of the organic connector resulted in enforcing this adsorption site. This may be crucial for improving the uptake properties of these materials to the goal defined by US Department of Energy for efficient hydrogen transport materials.

As far as we concered, there is no experimental and theoretical report about the adsorption of methane on MOFs. The main propose of the research is to calculate the adsorption of methane on different MOFs by *ab initio* and two-layered ONIOM methods. Theoretical absorption studies class of IRMOFs offer an useful information. Besides that, the study also gives the elementary information to bring the MOFs to become used as storage.

1.6 Scope of This Study

The objective of this study is to investigate the binding structures and energies between methane molecule and IRMOFs lattices using *ab initio* quantum chemical calculations. Several level of accuracies of the calculation methods as well as size of the fragment representing the IRMOF lattice were examined to seek for the optimal methode compromising between accuracy and time required.

CHAPTER II

THEORETICAL BACKGROUND

A basic understanding of how approximate molecular wave equations are constructed and solved is essential to the proper use of quantum chemical software. Quantum chemistry is highly mathematical in nature, and the language used to describe quantum chemical methods more often relates to equations than to chemical concepts. Non-specialists who are interested in using quantum chemical methods as molecular modeling tools can be faced with a considerable learning curve.

2.1 Quantum Chemistry

Quantum chemistry is a branch of theoretical chemistry, which applies quantum mechanics and quantum field theory to address issues and problems in chemistry. The description of the electronic behavior of atoms and molecules as pertaining to their reactivity is one of the applications of quantum chemistry. Quantum chemistry lies on the border between chemistry and physics, and significant contributions have been made by scientists from both fields. It has a strong and active overlap with the field of atomic physics and molecular physics, as well as physical chemistry.

Quantum chemistry mathematically describes the fundamental behavior of matter at the molecular scale[36]. It is, in principle, possible to describe all chemical systems using this theory. In practice, only the simplest chemical systems may realistically be investigated in purely quantum mechanical terms, and approximations must be made for most practical purposes (*e.g.*, Hartree-Fock, post Hartree-Fock or Density Functional Theory). Hence, a detailed understanding of quantum mechanics is not necessary for most chemistry, as the important implications of the theory can be understood and applied in simple terms.

2.2 Computational Chemistry

The term theoretical chemistry may be defined as a mathematical description of chemistry, whereas computational chemistry is usually used when a mathematical method is sufficiently well developed that it can be automated for implementation on a computer. Note that the words exact and perfect do not appear here, as very few aspects of chemistry can be computed exactly. However, almost every aspect of chemistry can be described in a qualitative or approximate quantitative computational scheme.

The methods employed cover both static and dynamic situations. In all cases the computer time increases rapidly with the size of the system being studied. That system can be a single molecule, a group of molecules or a solid. The methods are thus based on theories which range from highly accurate, but are suitable only for small systems, to very approximate, but suitable for very large systems. The accurate methods are used called *ab initio* methods, as they are based entirely on theory from first principles. The less accurate methods are called empirical or semi-empirical because some experimental results, often from atoms or related molecules, are used along with the theory

In theoretical chemistry, chemists, physicists and mathematicians develop algorithms and computer programs to predict atomic and molecular properties and reaction paths for chemical reactions. Computational chemists, in contrast, may simply apply existing computer programs and methodologies to specific chemical questions. There are two different aspects to computational chemistry:

- Computational studies can be carried out in order to find a starting point for a laboratory synthesis, or to assist in understanding experimental data, such as the position and source of spectroscopic peaks.
- Computational studies can be used to predict the possibility of so far entirely unknown molecules or to explore reaction mechanisms that are not readily studied by experimental means.

Thus, computational chemistry can assist the experimental chemist or it can challenge the experimental chemist to find entirely new chemical objects. Several major areas may be distinguished within computational chemistry:

- The prediction of the molecular structure of molecules by the use of the simulation of forces, or more accurate quantum chemical methods, to find stationary points on the energy surface as the position of the nuclei is varied.
- Storing and searching for data on chemical entities.
- Identifying correlations between chemical structures and properties.
- Computational approaches to help in the efficient synthesis of compounds.

2.3 *Ab initio* Methods

A quantum mechanic was first applied to molecules of real chemical systems, that dose not really on calibration against measured chemical parameters and it therefore called *ab initio*. The simplest type of *ab initio* electronic structure calculation is the Hartree-Fock (HF) approximation[36].

2.3.1 Hartree-Fock Method

The Hartree-Fock (HF) method is an approximate method for the determination of the ground-state wavefunction and ground-state energy of a quantum many-body system. The Hartree-Fock method assumes that the exact, N-body wavefunction of the system can be approximated by a single Slater determinant (in the case where the particles are fermions) or by a single permanent (in the case of bosons) of N spin-orbitals. Invoking the variational principle one can derive a set of N coupled equations for the N spin-orbitals. Solution of these equations yields the HF wavefunction and energy of the system, which are approximations of the exact ones.

The HF method finds its typical application in the solution of the electronic Schrödinger equation of atoms, molecules and solids but it has also found widespread use in nuclear physics. The rest of this article will focus on applications in electronic structure theory.

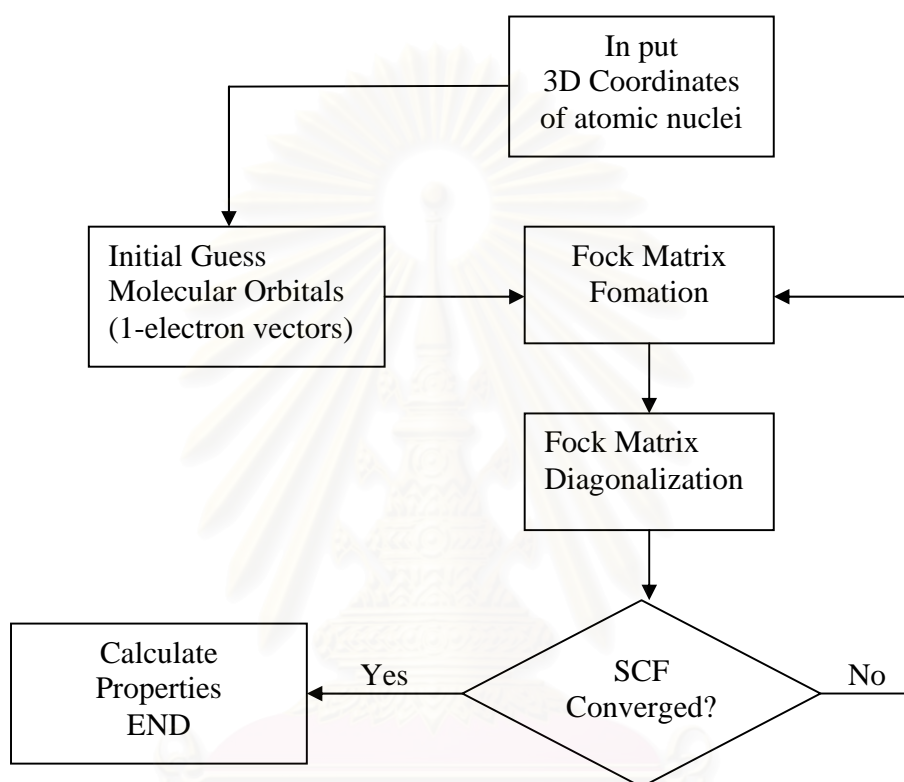


Figure 2.1 Flow chart of the HF procedure.

สถาบันวิทยบริการ
จุฬาลงกรณ์มหาวิทยาลัย

2.3.2 Møller-Plesset Perturbation Theory

Møller-Plesset perturbation theory (MP) is one of several quantum chemistry post-Hartree-Fock *ab initio* methods in the field of computational chemistry. It improves on the Hartree-Fock method by adding electron correlation effects by means of Rayleigh-Schrödinger perturbation theory (RS-PT), usually to second (MP2), third (MP3) or fourth (MP4) order[37].

Second (MP2), third (MP3), and fourth (MP4) order MP calculations are standard levels used in calculating small systems and are implemented in many computational chemistry codes. Systematic studies of MP perturbation theory have shown that it is not necessarily a convergent theory at high orders. The convergence properties can be slow, rapid, oscillatory, regular, highly erratic or simply non-existent, depending on the precise chemical system or basis set[38]. Additionally, various important molecular properties calculated at MP3 and MP4 level are in no way better than their MP2 counterparts, even for small molecules[39].

2.4 Density Functional Theory Methods

Density Functional Theory (DFT) methods are often considered to be *ab initio* methods for determining the molecular electronic structure, even though many of the most common functionals use parameters derived from empirical data, or from more complex calculations. This means that they could also be called semi-empirical methods. It is best to treat them as a class on their own. In DFT, the total energy is expressed in terms of the total one-electron density rather than the wave function. In this type of calculation, there is an approximate Hamiltonian and an approximate expression for the total electron density. DFT methods can be very accurate for little computational cost. The drawback is that, unlike *ab initio* methods, there is no systematic way to improve the methods by improving the form of the functional. Some methods combine the density functional exchange functional with the HF exchange term and are known as hybrid functional methods.

2.5 Semi-empirical Methods

Semi-empirical methods follow what are often called empirical methods are based on the HF formalism[36], but make many approximations and obtain some parameters from empirical data. They are very important in computational chemistry for treating large molecules where the full HF method without the approximations is too expensive. The use of empirical parameters appears to allow some inclusion of electron correlation effects into the methods.

Semi-empirical calculations are much faster than their *ab initio* counterparts. Their results, however, can be very wrong if the molecule being computed is not similar enough to the molecules in the database used to parametrize the method. Semi-empirical calculations have been most successful in the description of organic chemistry, where only a few elements are used extensively and molecules are of moderate size.

2.5.1 AM1 Method

Austin Model 1 (AM1) is a semi-empirical method for the quantum calculation of molecular electronic structure in computational chemistry. It is based on the Neglect of Differential Diatomic Overlap integral approximation. Specifically, it is a generalization of the modified neglect of differential diatomic overlap approximation.

AM1 is an attempt to improve the MNDO (Modified neglect of differential overlap) model by reducing the repulsion of atoms at close separation distances. The atomic core-atomic core terms in the MNDO equations were modified through the addition of off-center attractive and repulsive Gaussian functions. The complexity of the parameterization problem increased in AM1 as the number of parameters per atom increased from 7 in MNDO to 13-16 per atom in AM1. The results of AM1 calculations are sometimes used as the starting points for parameterizations of forcefields in molecular modelling.

2.5.2 PM3 Method

Parameterized Model number 3 (PM3) is a semi-empirical method for the quantum calculation of molecular electronic structure in computational chemistry. It is based on the Neglect of Differential Diatomic Overlap integral approximation.

The PM3 method uses the same formalism and equations as the AM1 method[40]. PM3 uses two Gaussian functions for the core repulsion function, instead of the variable number used by AM1 the numerical values of the parameters are different. The other differences lie in the philosophy and methodology used during the parameterization: whereas AM1 takes some of the parameter values from spectroscopical measurements, PM3 treats them as optimizable values.

2.6 Basis Set

A basis set in chemistry is a set of functions used to create the molecular orbitals, which are expanded as a linear combination of such functions with the weights or coefficients to be determined. Usually these functions are atomic orbitals, in that they are centered on atoms, but functions centered in bonds or lone pairs have been used as have pairs of functions centered in the two lobes of a p orbital. Additionally, basis sets composed of sets of plane waves down to a cutoff wavelength are often used, especially in calculations involving systems with periodic boundary conditions.

2.6.1 Minimal Basis Sets

The most common minimal basis set is STO-nG, where n is an integer. This n value represents the number of Gaussian primitive functions comprising a single basis function. In these basis sets, the same number of Gaussian primitives comprise core and valence orbitals. Minimal basis sets typically give rough results that are insufficient for research-quality publication, but are much cheaper than their larger counterparts. Commonly used minimal basis sets of this type are:STO-3G/STO-4G/STO-6G and STO-3G* - Polarized version of STO-3G

2.6.2 Split-valence basis sets

During most molecular bonding, it is the valence electrons which principally take part in the bonding. In recognition of this fact, it is common to represent valence orbitals by more than one basis function, basis sets in which there are multiple basis functions corresponding to each valence atomic orbital, are called valence double, triple, or quadruple-zeta basis sets. Since the different orbitals of the split have different spatial extents, the combination allows the electron density to adjust its spatial extent appropriate to the particular molecular environment. Minimum basis sets are fixed and are unable to adjust to different molecular environments. Basis sets in which there are multiple basis functions corresponding to each atomic orbital, including both valence orbitals and core orbitals are called double, triple, or quadruple-zeta basis sets.

2.6.3 Polarization Functions

Polarized basis sets allow some small contributions from the unfilled orbital, what is required for the ground state for atom description by adding orbitals with angular momentum beyond. Pople and co-workers introduced a simple nomenclature scheme to indicate the presence of these functions, the “*” (star). Thus, 6-31G* implies a set of *d* functions added to polarized the *p* functions in 6-31G. A second star implies *p* functions on H and He, *e.g.*, 6-31G**. To use more than one set of polarization functions in modern calculation, the standard nomenclature for the Pople basis sets now typically includes an explicit enumeration of those functions instead of the star nomenclature.

2.6.4 Diffuse Functions

When a basis set does not have the flexibility necessary to allow a weakly bound electron to localize far from the remaining density (such as molecules with lone pairs, anions and other systems with significant negative charge, systems in their excited states,

and system with low ionization potentials), significant errors in energies and other molecular properties can occur. In the Pople family of basis sets, the presence of diffuse functions is indicated by a “+” in the basis set name. The 6-31G+* indicates that heavy atoms have been augmented with an additional one *s* and one set of *p* functions having small exponents.

2.7 Basis Set Superposition Error

In quantum chemistry, calculations of interaction energies are susceptible to basis set superposition error (BSSE) if they use finite basis sets. As the atoms of interacting molecules (or of different parts of the same molecule) or two molecules approach one another, their basis functions overlap. Each monomer “borrows” functions from other nearby components, effectively increasing its basis set and improving the calculation of derived properties such as energy. If the total energy is minimised as a function of the system geometry, the short-range energies from the mixed basis sets must be compared with the long-range energies from the unmixed sets, and this mismatch introduces an error.

2.8 ONIOM Method

ONIOM (Our N-layer Integrated molecular Orbital + molecular Mechanics) method was developed in Morokuma group[41-46], allows the user to partition a chemical system into layers, which can then each be treated at a different level of theory are applied to different parts of a molecule. A molecule system can be divided into up to three layers and the three layers do not have to be inclusive, provides a possibility to achieve such high accuracy calculation on a large molecular system. The active part of the reaction is considered in the “model” system and is treated with both at “high” and “low” levels of molecular Orbital calculation, whereas the entire “real” system is treated only at the “low” level of molecular Orbital calculation, and then they are integrated to define the ONIOM total energy of the “real” system. ONIOM is a computationally efficient tool for the study of chemical reactions involving large molecular systems.

2.9 GAUSSIAN Program

GAUSSIAN is a computational chemistry software program, first written by John Pople[47]. Gaussian's copyright was originally held by Carnegie Mellon University, and later by Gaussian Inc. Gaussian quickly became a popular and widely-used electronic structure program, including cutting-edge research in quantum chemistry and other fields. Applications of Gaussian functions appear in many contexts in the natural sciences, the social sciences, mathematics, and engineering. Some examples include:

- In statistics and probability theory, Gaussian functions appear as the density function of the normal distribution, which is a limiting probability distribution of complicated sums, according to the central limit theorem.
- A Gaussian function is the wave function of the ground state of the quantum harmonic oscillator.
- The molecular orbitals used in computational chemistry can be linear combinations of Gaussian functions called Gaussian orbitals.
- Mathematically, the derivatives of the Gaussian function are used to define Hermite polynomials.
- Consequently, Gaussian functions are also associated with the vacuum state in quantum field theory.
- Gaussian beams are used in optical and microwave systems.
- Gaussian functions are used as smoothing kernels for generating multi-scale representations in computer vision and image processing. Specifically, derivatives of Gaussians are used as a basis for defining a large number of types of visual operations.
- Gaussian functions are used in some types of artificial neural networks.

CHAPTER III

CALCULATION DETAILS

In this chapter, interaction energies of methane-benzene derivatives and methane-IRMOFs complexes were carried out using several methods of *ab initio* calculations. The GAUSSIAN03 package[47] was used for all calculations.

3.1 Interaction Between Methane Molecule and Aromatic Systems

The effects of functional groups on the weak interaction between methane molecule and aromatic- π system have been studied using quantum chemical calculations at several levels of accuracy. In the MOFs system, such small functional groups were found to play a key role in the guest-host interaction and, hence, their applications as the hydrocarbon storage and adsorption. Here, the simple models of benzene-derivatives, which are benzene, fluorobenzene, cyanobenzene, phenol, aniline and xylene molecules were used to represent the aromatic- π system. Those molecules are commonly found as the linker part of the MOFs. Therefore, the calculated systems consist of one methane molecule and benzene or benzene derivatives.

The *ab initio* methods, HF, DFT(B3LYP) and MP perturbation were used to optimize geometries and calculate binding energies of the $\text{CH}_4\text{-C}_6\text{H}_6$ and its derivatives $\text{CH}_4\text{-C}_6\text{H}_5\text{X}$ ($\text{X} = \text{F}, \text{CN}, \text{OH}, \text{NH}_2$ and CH_3) complexes. Three basis sets, 6-31G*, 6-31G** and 6-31+G* were applied to observe their effect on both structural and energetic properties of the complexes. In order to reduce the scope of the calculation, the methane molecule was assigned to approach to host molecules in the two orientations, H-in and H-out as shown in Figure 3.1.

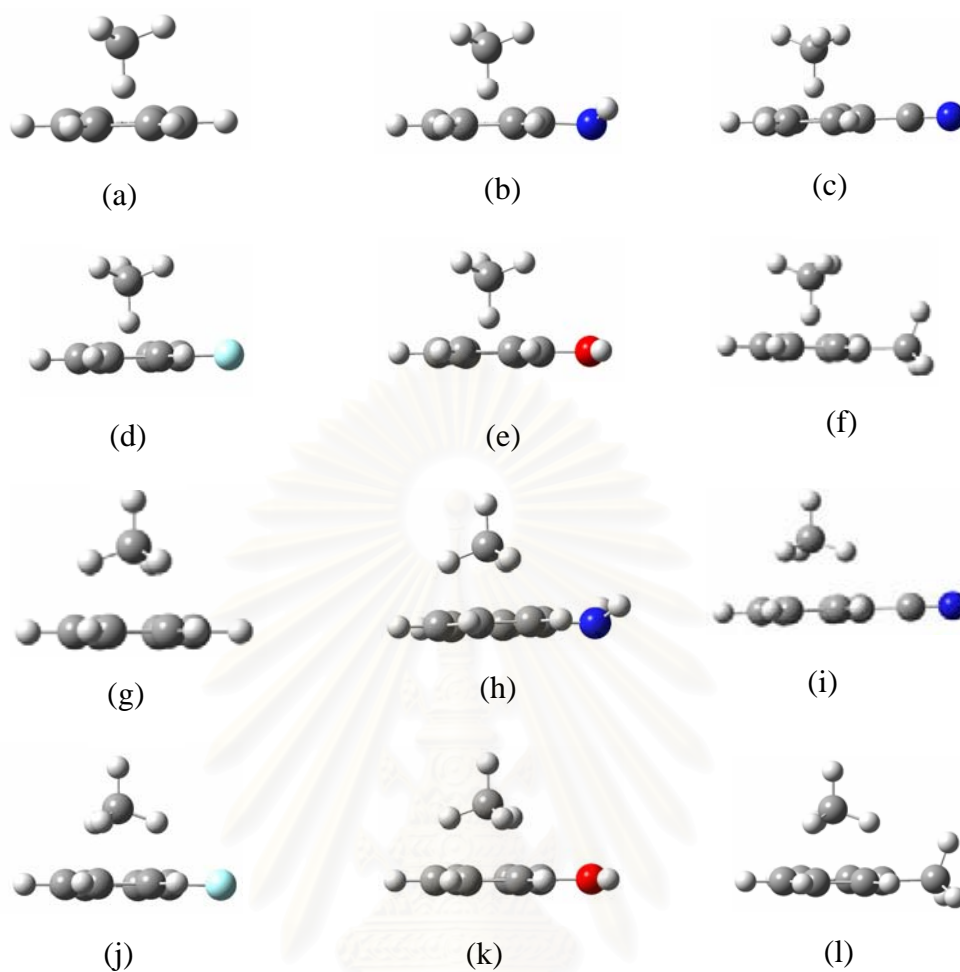


Figure 3.1 Twelve different models to investigate binding energies between CH_4 and benzene derivatives, (a),(g) benzene; (b),(h) aniline; (c),(i) cyanobenzene; (d),(j) fluorobenzene; (e),(k) phenol and (f),(l) xylene, where CH_4 molecule are in H-in (a-f) and H-out (g-l).

The binding energy of the complex, ΔE_{cpx} , is defined as the energy difference between the optimized complex and a summation of its monomer energies as shown in equation 3.1,

$$\Delta E_{bind} = E_{cpx} - E_g - E_s \quad (3.1)$$

Where, E_{cpx} is the total energy of the complex while E_g and E_s are the total energies of the guest molecule and the fragment-surface, respectively. Basis set superposition error (BSSE) was corrected using the counterpoise procedure [48].

3.2 Initial Structure of IRMOFs Lattice

3.2.1 IRMOF-1

The unit cell of IRMOF-1 (Figure 3.2b) is too large for the calculation of every possible configuration of the complex. In order to make the calculation practically possible, a column consisting of two corners connected by a linker, $(\text{Zn}_4\text{O})_2(\text{COOCH}_3)_{10}(\text{COO})_2\text{C}_6\text{H}_4$, was generated (Figure 3.2a). It was, then, used as starting structure.

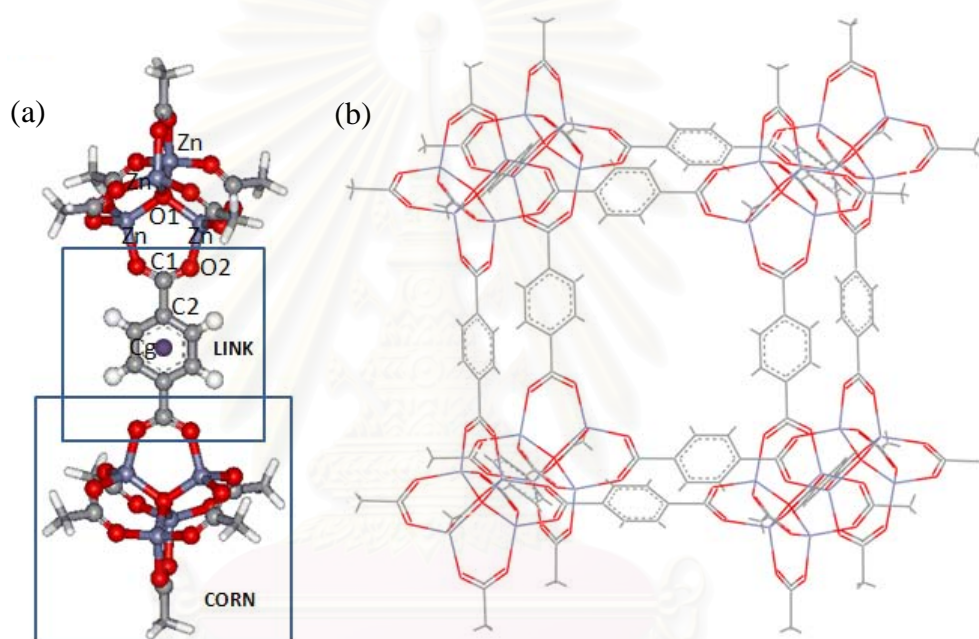


Figure 3.2 (a) A single linker of the IRMOF-1 consisting of two corners and one linker and (b) The IRMOF-1 unit cell.

The IRMOF-1 was represented by the three models shown in Figure 3.3. The fragments consisting of 1, 2 and 3 columns were named, for simplicity, as SINGLE, DOUBLE and TRIPLE, respectively.

To calculate interaction energy between CH_4 molecule and the linker (LINK), guest molecules were generated to move along the vector perpendicular to the molecular plane of the benzene ring at the C_g (see Figure 3.1a for definition).

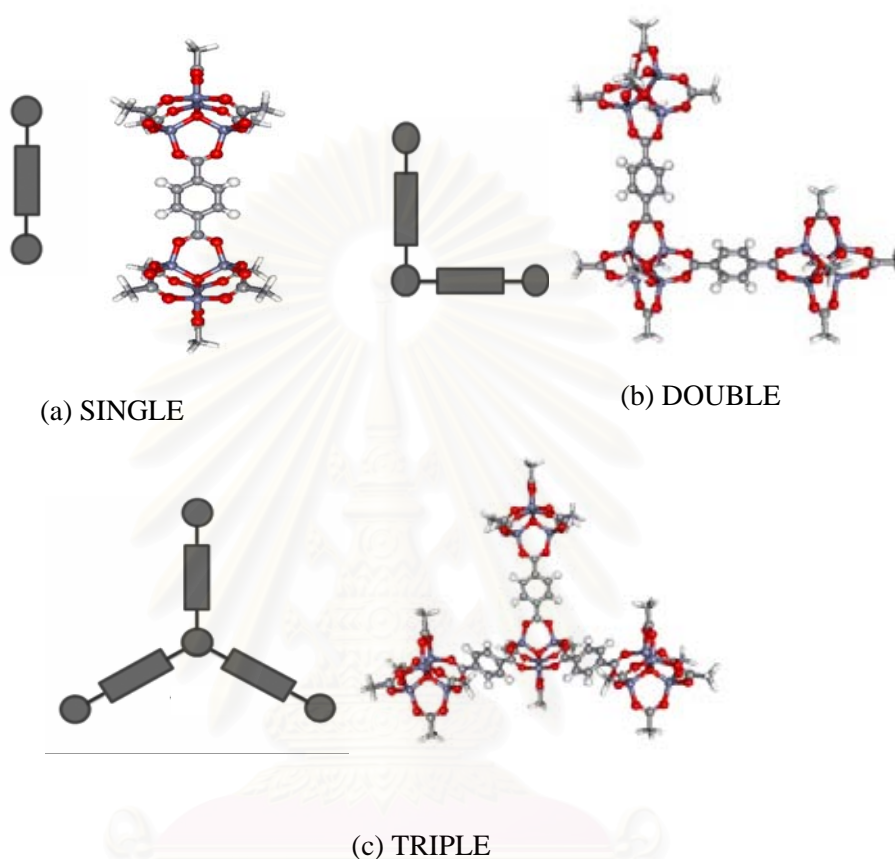


Figure 3.3 Models SINGLE, DOUBLE and TRIPLE represent the IRMOF-1 fragments containing one, two and three units as oriented, respectively.

For the SINGLE, DOUBLE and TRIPLE models, calculations were carried out only for one wing of the fragments. Here, two possible orientations of guest molecules were taken into account, H-in and H-out to the IRMOF-1 fragments as shown in Figure 3.4. Precisely, H-in and H-out for CH_4 means that it points one H atom forward and backward the IRMOF fragment, respectively. For the MOF corner (CORN), guest molecules, also in the two configurations, were generated to move along the vector pointing to O_1 (see Figure 3.2a).

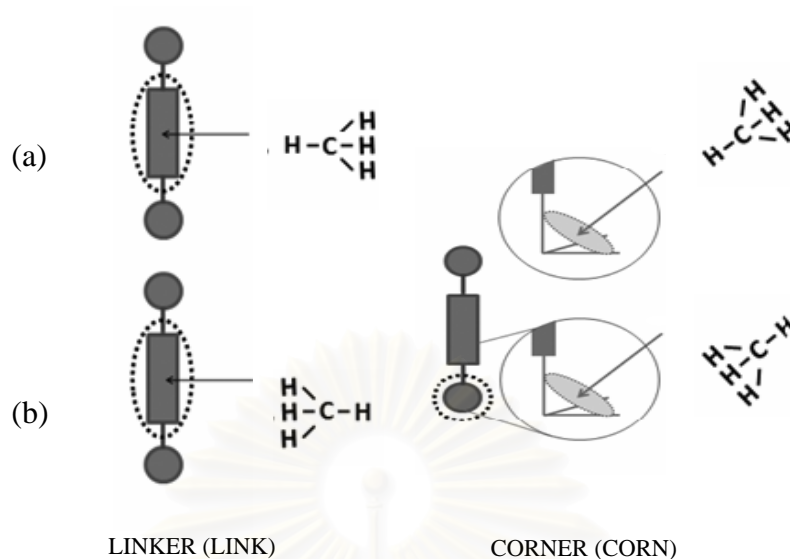


Figure 3.4 Orientation of methane molecules in (a) H-in orientation and (b) H-out orientation to the binding site (linker or corner).

Subsequently, the interaction energies of the above mentioned configurations were calculated using ONIOM method with BSSE corrections. The method used for the high (model) : low (real) levels was represented by MP2/6-31G** : HF/6-31G**. The model MP2/6-31G** part covers the compositions (C_6H_4) and the $(\text{Zn}_4\text{O})(\text{CO}_2)_6$ for the linker and corner domains, respectively, labeled as ball and stick see in Figure 3.5. The real parts were the whole SINGLE, DOUBLE and TRIPLE fragments.

สถาบันวิทยบริการ
จุฬาลงกรณ์มหาวิทยาลัย

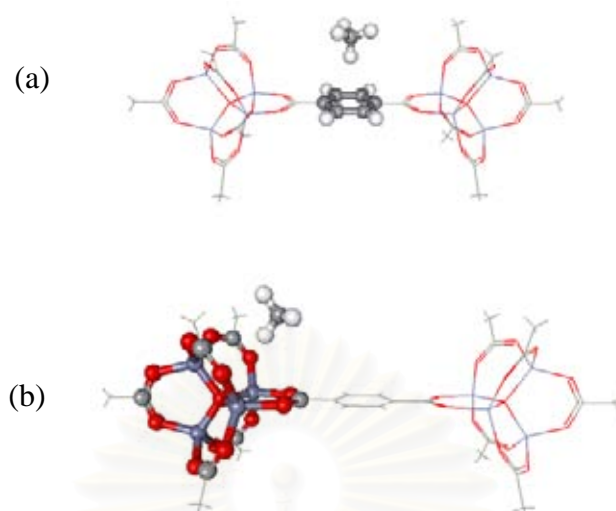


Figure 3.5 The real part (line) and the model part (ball and stick) for the ONIOM method of IRMOF-1, (a) at the linker and (b) at the corner.

The ONIOM interaction energy of the system, ΔE_{ONIOM} can be estimated from the following three independent calculations:

$$\Delta E_{ONIOM} = E_{(real, low)} + E_{(model, high)} - E_{(model, low)} \quad (3.2)$$

Where $E_{(real, low)}$ is the total energy of the real system using the low level method, while $E_{(model, high)}$ and $E_{(model, low)}$ denote the total energies of the model part calculated with high and low level methods, respectively.

The binding energy is defined according to the supermolecular approach as shown in equation 3.1.

3.2.2 IRMOF-6

In the IRMOF series developed by Yaghi *et al.*[3], the basic structural motif of $Zn_4O(CO_2)_6$ clusters as secondary building unit (SBUs) connected by aromatic phenyl-containing linkers is repeated to generate a series of isostructural materials. They differ only in the central portion of the ligand[3,49]. IRMOF-6 can be generated by changing the linker from simple phenyl ring (MOF-5/IRMOF-1) to be cyclobutylbenzene (IRMOF-6). A column of IRMOF-6 consisting of two corners connected by a linker, $(Zn_4O)_2(COOCH_3)_{10}(COO)_2C_8H_6$, was generated and shows in the Figure. 3.6a. It was, then, used as starting structure.

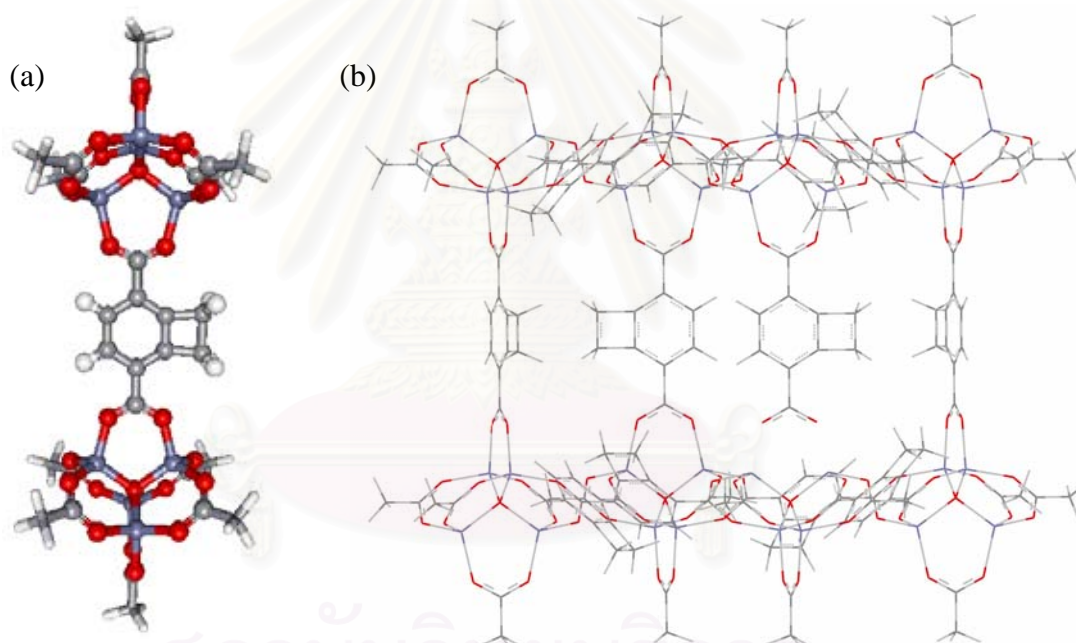


Figure 3.6 (a) A single linker of the IRMOF-6 consisting of two corners and one linker (cyclobutylbenzene) and (b) The IRMOF-6 unit cell.

The SINGLE DOUBLE and TRIPLE models for IRMOF-6 are defined linker to these of the IRMOF-1 (see section 3.2.1). As shows in Figure 3.7, there are two possible configurations of the cyclobutylbenzene for the DOUBLE and TRIPLE

clusters, model I and II is Figure 3.7b and Figure 3.7c. For the orientations of guest molecule, H-in and H-out the same as the IRMOF-1 configurations are used Figure 3.7. Also similar to those in the IRMOF-1, guest molecule generated to move along the vector pointing to O_1 (see Figure 3.2a).

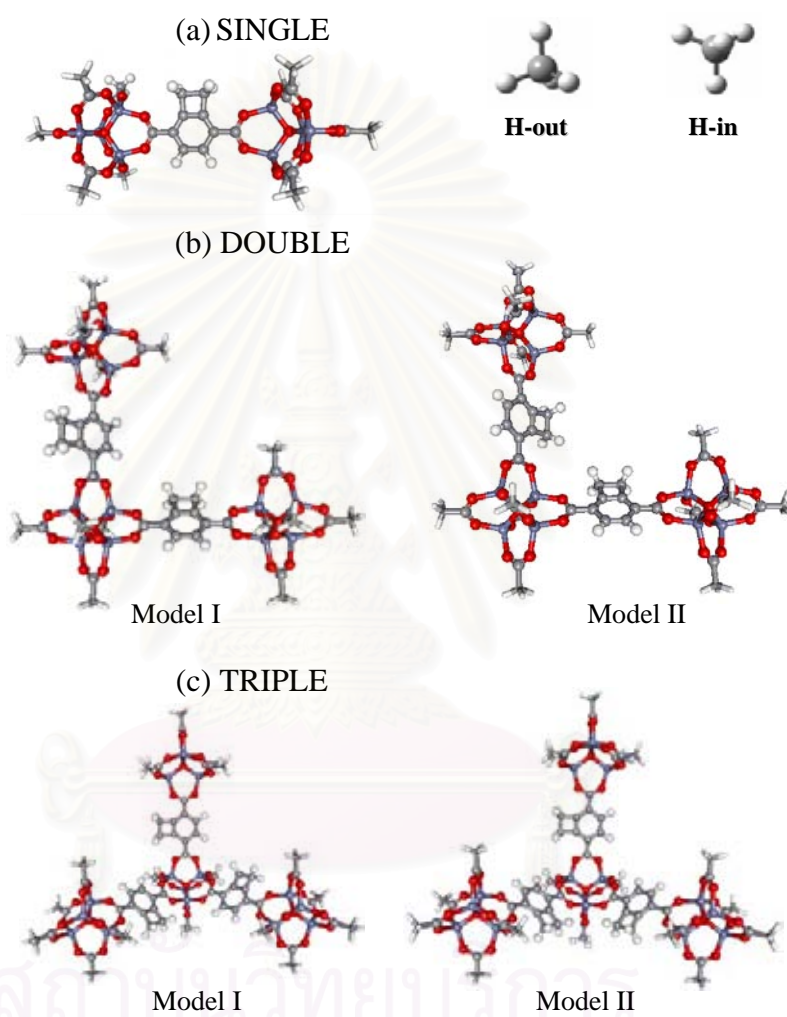


Figure 3.7 Models SINGLE, DOUBLE (Models I, II) and TRIPLE (Models I, II) represent the IRMOF-6 fragments containing one, two and three units as oriented, respectively.

The interaction energies for the above mentioned configurations were calculated using ONIOM(MP2/6-31G**: $\text{HF}/6\text{-}31\text{G}^{**}$) method with BSSE corrections. Figure 3.8 shows the model part (ball-and-stick) and the real part (line) for the ONIOM calculations.

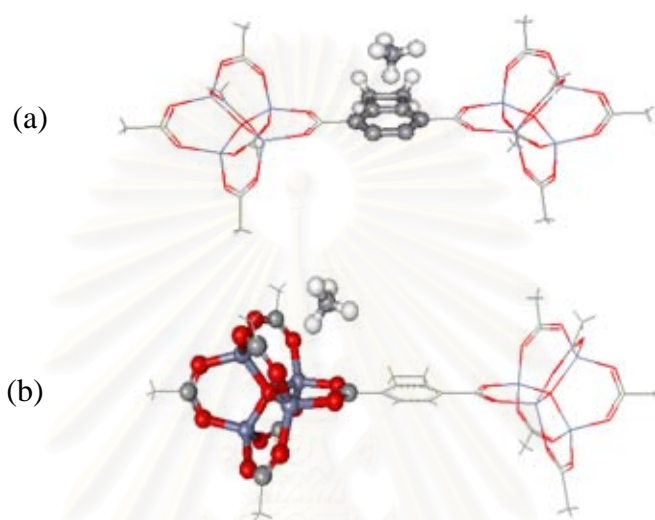


Figure 3.8 The real part (line) and the model part (ball and stick) for the ONIOM method of IRMOF-6, (a) at the linker and (b) at the corner.

3.2.3 IRMOF-14

IRMOF-14 is a member of IRMOFs series, consists of zinc oxide clusters connected by pyrenedicarboxylate (PDC) linkers. A column consisting of two corners connected by a linker, $(\text{Zn}_4\text{O})_2(\text{COOCH}_3)_{10}(\text{COO})_2\text{C}_{16}\text{H}_8$, was generated as shown in the Figure. 3.9a. It was then, used as starting structure.

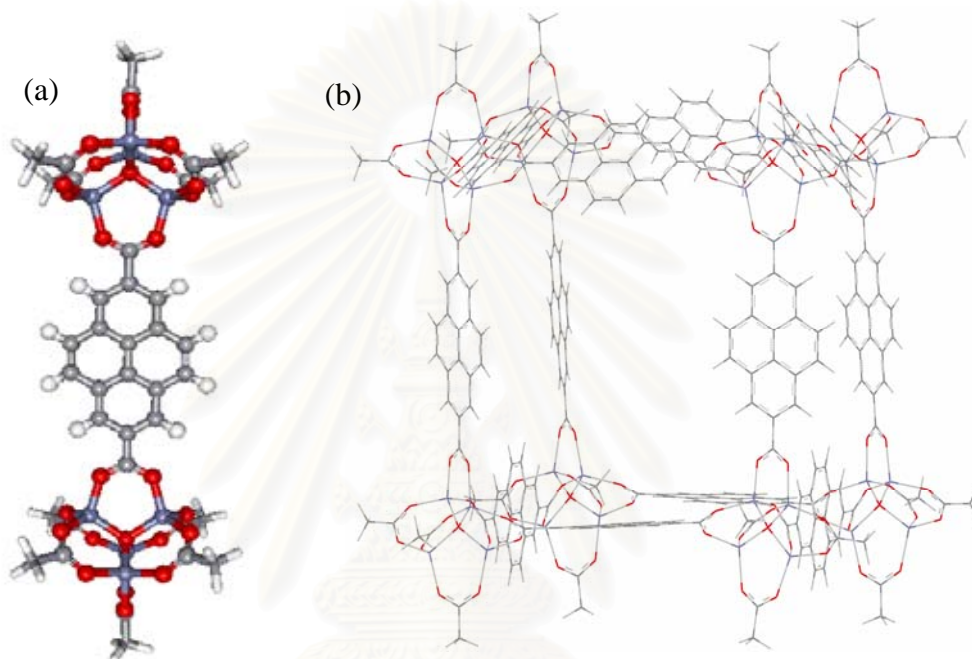


Figure 3.9 (a) A single linker of the IRMOF-14 consisting of two corners and one linker (b) The IRMOF-14 unit cell.

The SINGLE, DOUBLE and TRIPLE models, were defined in the same manner at IRMOF-1. Based on molecular symmetry, different binding sites (model I-II for SINGLE and models I-III for DOUBLE and TRIPLE) were defined according to Figure 3.10. Again, two configurations of CH₄ are taken into account. The Figure 3.11 shows the model part (ball-and-stick) and the real part (line) for the ONIOM (MP2/6-31G**: $\text{HF}/6-31\text{G}^{**}$) calculations.

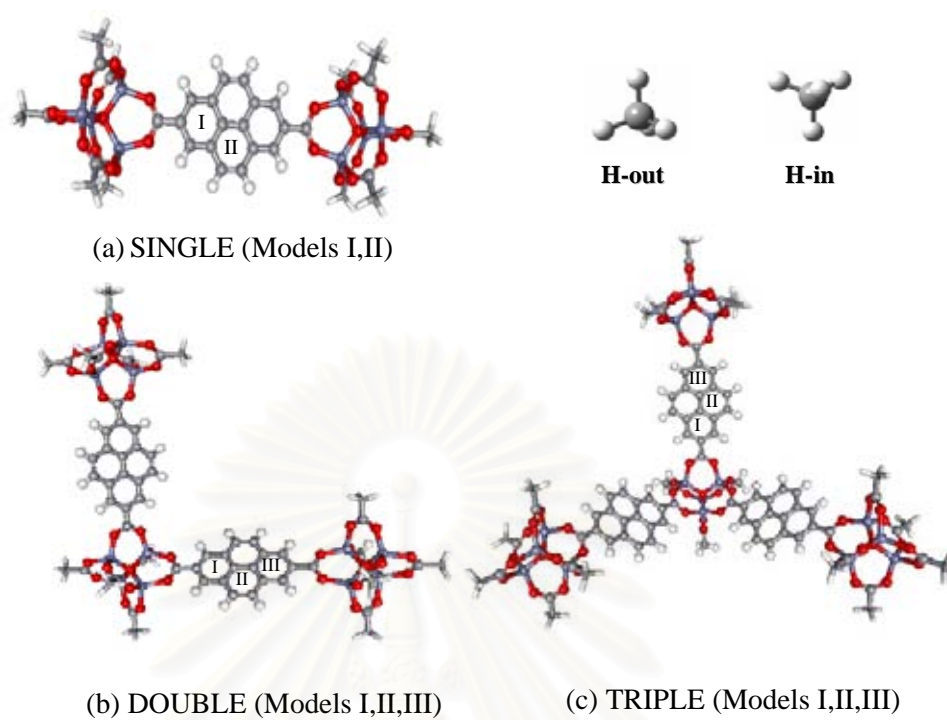


Figure 3.10 Models SINGLE (Models I, II) and DOUBLE, TRIPLE (Models I, II,III) represent the IRMOF-14 fragments.

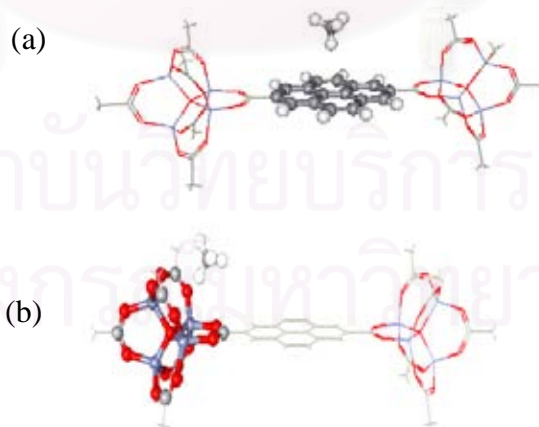


Figure 3.11 The real part (line) and the model part (ball and stick) for the ONIOM method of IRMOF-14, (a) at the linker and (b) at the corner.

CHAPTER IV

RESULTS AND DISCUSSIONS

4.1 Interaction Between Methane Molecule and Aromatic Systems

The calculations of methane-benzene and methane-benzene derivatives complexes were carried out, aimed to understand the effects of functional groups on the weak interaction between CH_4 and aromatics- π systems. This interaction was known to play important role on the adsorption processes of hydrocarbon guest molecules in the IRMOFs lattices. The binding energies of all complexes described in CHAPTER III at several levels of calculations were summarized in Table 4.1 and plotted in Figure 4.2. The optimal structures obtained from the HF, B3LYP and MP2 methods using the 6-31G** basis set were shown in Figure 4.1.

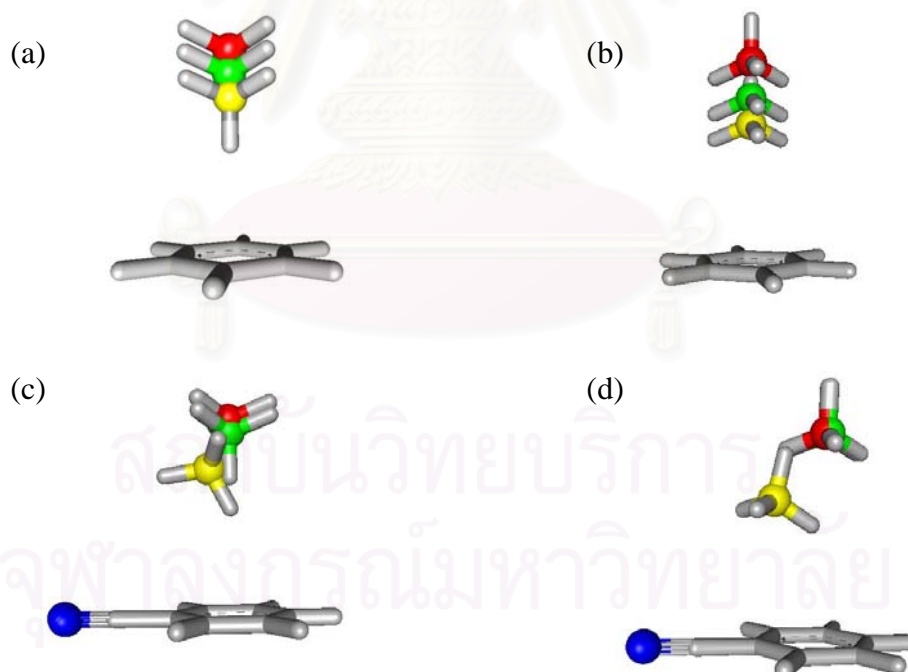


Figure 4.1 Optimized structures of $\text{CH}_4\text{-C}_6\text{H}_6$ (a, b) and $\text{CH}_4\text{-C}_6\text{H}_5\text{CN}$ (c, d) with the starting configurations H-in (a, c) and H-out (b, d). The yellow (●), red (●) and green (●) balls are the carbon atoms obtained from the MP2, HF and B3LYP at the 6-31G** basis set, respectively.

Table 4.1 The binding energies (kJ/mol) with the BSSE corrections of the optimized CH₄-C₆H₆ complex and its derivatives CH₄-C₆H₅X (X = F, CN, OH, NH₂ and CH₃).

Basis Set	HF		B3lyp		MP2	
	H-in	H-out	H-in	H-out	H-in	H-out
Benzene						
6-31G+*	-0.23	0.12	0.77	0.93	-1.85	-1.58
6-31G**	-0.07	0.93	0.66	1.91	-1.54	-0.81
6-31G*	-0.08	0.92	1.09	1.84	1.25	-0.42
Aniline						
6-31G+*	-0.29	0.15	0.22	0.28	-2.65	-1.83
6-31G**	-0.13	1.06	0.51	2.18	-1.86	-0.88
6-31G*	-0.11	1.05	4.69	7.10	-1.53	-0.47
Cyanobenzene						
6-31G+*	0.01	0.07	0.67	0.07	-2.54	-2.59
6-31G**	0.17	0.69	0.64	0.69	-1.68	-1.92
6-31G*	0.16	0.58	0.68	0.58	-1.45	-1.51
Fluorobenzene						
6-31G+*	-0.10	0.09	0.53	0.17	-2.10	-1.91
6-31G**	0.07	0.78	0.65	1.45	-1.34	-0.49
6-31G*	0.06	0.76	0.55	1.92	-1.06	-0.29
Phenol						
6-31G+*	-0.16	0.11	0.37	0.14	-2.34	-2.64
6-31G**	-0.02	0.81	0.56	0.41	-1.68	-0.80
6-31G*	-0.03	0.79	0.48	0.25	-1.27	-0.63
Xylene						
6-31G+*	-0.25	0.07	0.33	0.10	-2.50	-2.54
6-31G**	-0.11	0.69	0.46	1.56	-2.03	-1.96
6-31G*	-0.10	0.67	0.42	1.74	-1.59	-1.58

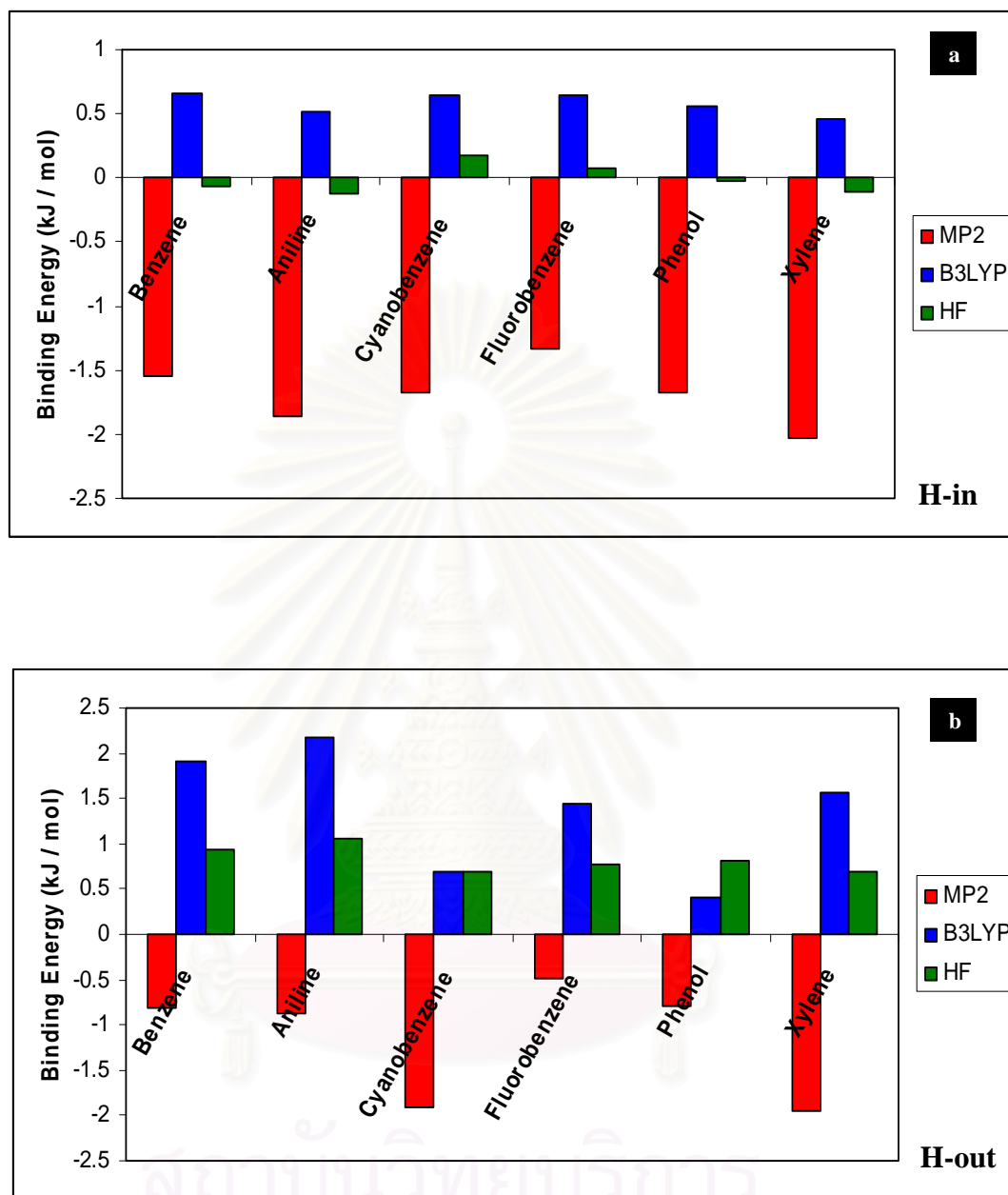


Figure 4.2 The binding energies between CH₄ and benzene derivatives at the optimal structures using MP2/6-31G**.

It can be seen from Table 4.1 and Figure 4.2 that among the three methods (HF, B3LYP and MP2) at the same basis set, the binding energies of all complexes are in the following order $MP2 < HF < B3LYP$. It is known that the calculated results depend strongly on the used method especially for the weak interaction systems. Previous study shown that DFT/B3LYP method failed to estimate the interaction energy with π -electron clouds [48].

The MP2/6-31G+* for the methane-benzene derivatives give lowest interaction energy. Due to the fact that the MP2/6-31G+* is highly time consuming, it is practically impossible to apply it for the large system. Therefore, the optimal choice shifts to the next lower-accurate MP2/6-31G** methods. The binding energies between methane and benzene-derivatives obtained from the MP2/6-31G** method, were sorted by their stabilities from high to low as aniline, cyanobenzene, phenol, xylene, fluorobenzene and benzene, respectively. Effect of functional group can be clearly seen not only in terms of binding energies but also in the optimal configuration of the complexes (Figure 4.2.).

Since the CH/ π bonding is mainly determined by the correlation energy, the binding is weak, and Van der Waals interactions are important, therefore, the standard DFT and HF calculations are not suitable for such system. By contrast, MP2 theory is known to provide more accurate results. Due to the constraints in computational resources, the MP2 calculations can also performed only on small model system. Large basis sets are necessary to provide the required accuracy for these calculations.

4.2 Geometries of the IRMOF-1

Starting from the SINGLE linker (Figure 3.2a) and the whole unit cell (Figure 3.2b) of the IRMOF-1, the properties of the optimal structures obtained from several methods are summarized in Table 4.2. In the case of SINGLE linker structure the MPW1PW91/6-31G** methods yielded an overall structure in very good agreement with the experimental data[3]. However, the MPW1PW91/6-31G** method was highly time consuming. Therefore, it was practically not possible to apply to the full unit-cell cluster. In the case of a unit cell, the choice of the method shifted to the next lower accurate B3LYP/6-31G**. The semi-empirical methods AM1 and PM3 were carried out for comparison. As expected, these two methods yield the structural data for the SINGLE linker and the unit cell far from those observed experimental data.



Table 4.2 The bond distances and bond angles obtained from the geometry optimizations as shown in Figure 3.2a.

Method/basis set	Bond length (pm)				Bond angle (°)		
	Zn-O ₁	Zn-O ₂	O ₂ -C ₁	C ₁ -C ₂	O ₁ -Zn-O ₂	Zn-O ₂ -C ₁	O ₂ -C ₁ -C ₂
<i>a.) One column cluster (Figure 3.2a)</i>							
AM1	205.5	212.4	128.5	148.5	110.1	134.2	119.0
PM3	195.1	205.3	127.6	150.7	112.4	131.2	118.2
HF/6-31G*	197.8	196.9	124.5	149.7	110.1	132.8	117.7
HF/6-31G**	197.8	196.9	124.5	149.7	110.1	132.8	117.7
B3LYP/6-31G*	195.4	195.0	127.0	149.6	111.2	131.1	117.2
B3LYP/6-31G**	195.3	195.1	127.0	149.6	111.1	131.2	117.2
B3LYP/6-311G**	196.1	195.7	126.4	149.6	109.7	131.1	117.3
B3LYP/6-311G** [49]	197.2	195.3	126.2	151.0	110.8	131.7	117.8
MPW1PW91/6-31G**	194.0	194.0	126.4	149.1	111.2	131.0	117.2
<i>b.) One unit cell cluster (Figure 3.2b)</i>							
AM1	205.4	212.1	128.5	148.5	110.2	134.2	119.0
PM3	195.1	205.4	127.5	150.7	112.1	130.7	117.6
B3LYP/6-31G**	195.3	194.8	127.0	149.6	111.4	131.1	117.3
Experimental data[3]	193.6	194.1	125.2	149.8	111.1	132.3	118.1

4.3 Interaction of CH₄ in IRMOF-1 and Effect of BSSE

Adsorption of methane on IRMOF-1 was investigated using various sizes of clusters, which the smallest model consists of (Zn₄O)₂(COOCH₃)₁₀(COO)₂C₆H₄. There are two possible sites within the IRMOFs lattice, at the linker and the corner. Since a unit cell of IRMOFs is too large, so it can not be directly apply for quantum chemical calculation, therefore, the calculations were carried out for different sizes of the models, SINGLE, DOUBLE and TRIPLE. The results obtained from the ONIOM (MP2/6-31G**:^{HF2}/6-31G**) calculations for changes of the binding energies as a function of separation were given in Figures 4.3-4.8., the linker and corner were summarized in Tables 4.3 and 4.4, respectively.

Table 4.3 ONIOM binding energies with and without BSSE corrections and the corresponding distances between IRMOF-1 linker in the three cluster models (SINGLE, DOUBLE and TRIPLE) and CH₄ molecule.

Model		Distance Cg-C (Å)		Binding energy (kJ/mol)	
IRMOF-1	CH ₄	With BSSE	Without BSSE	With BSSE	Without BSSE
SINGLE	H-in	4.08	3.73	-2.15	-6.19
	H-out	3.97	3.63	-1.86	-5.01
DOUBLE	H-in	4.09	3.73	-2.17	-6.19
	H-out	3.98	3.63	-1.84	-5.01
TRIPLE	H-in	4.10	3.73	-2.15	-6.19
	H-out	3.98	3.64	-1.83	-5.01

Table 4.4 ONIOM binding energies with and without BSSE corrections and the corresponding distances between IRMOF-1 corner in the three cluster models (SINGLE, DOUBLE and TRIPLE) and CH₄ molecule.

Model		Distance O ₁ -C (Å)		Binding energy (kJ/mol)	
IRMOF-1	CH ₄	With BSSE	Without BSSE	With BSSE	Without BSSE
SINGLE	H-in	4.92	4.19	-3.18	-12.11
	H-out	4.90	4.42	-3.64	-12.66
DOUBLE	H-in	4.90	4.16	-3.11	-12.31
	H-out	4.91	4.43	-3.74	-12.57
TRIPLE	H-in	4.92	4.26	-3.00	-11.89
	H-out	4.90	4.41	-3.80	-12.95

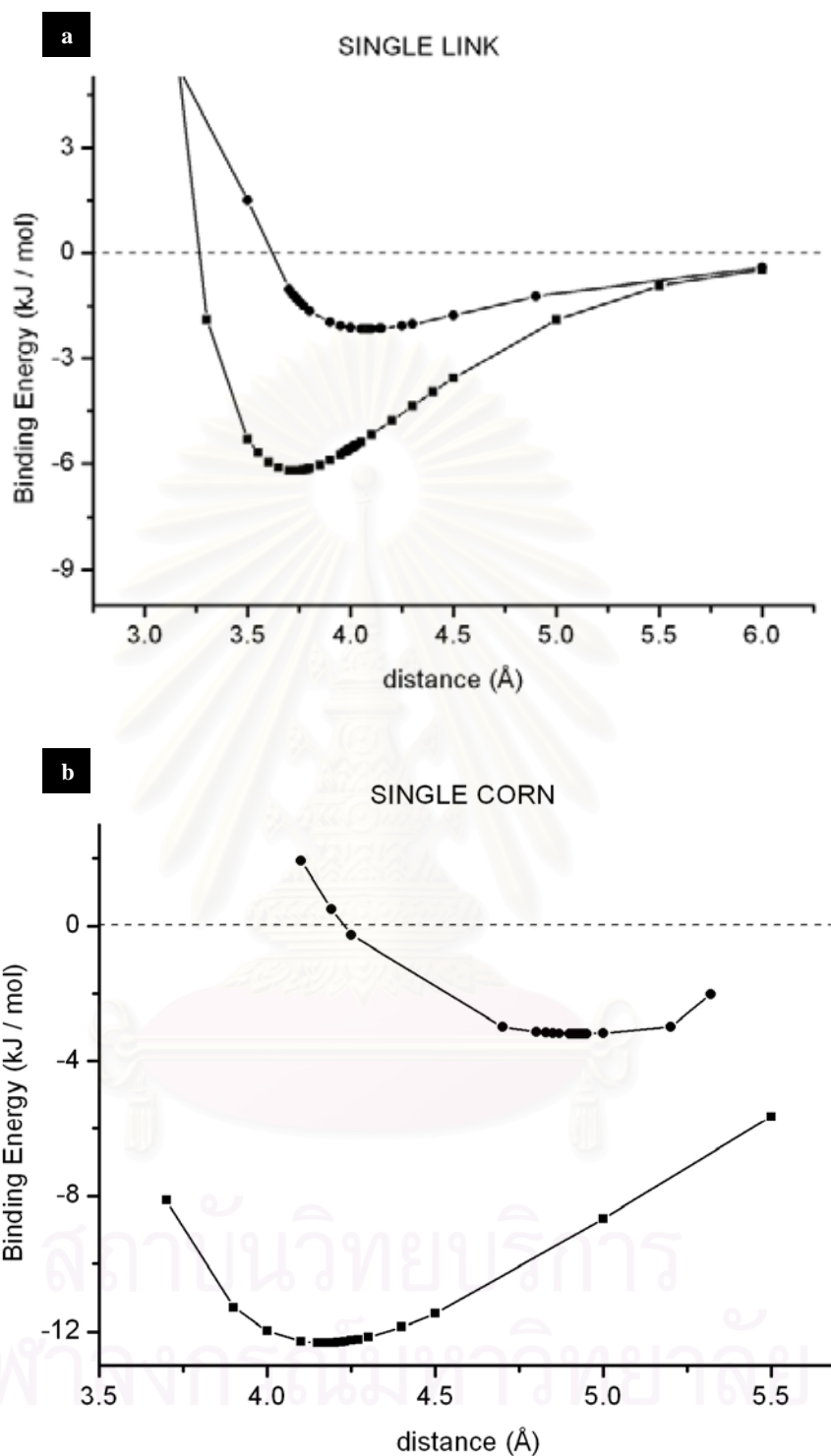


Figure 4.3 ONIOM binding energies (●) with BSSE and (■) without BSSE corrections for the $\text{CH}_4/\text{MOF-5}$ complexes where CH_4 was located in the H-in configuration (a) for the SINGLE linker (LINK) and (b) for the SINGLE corner (CORN) calculations, the distances were measured from the C atom of CH_4 to Cg and O_1 , respectively (see Figure 3.2a).

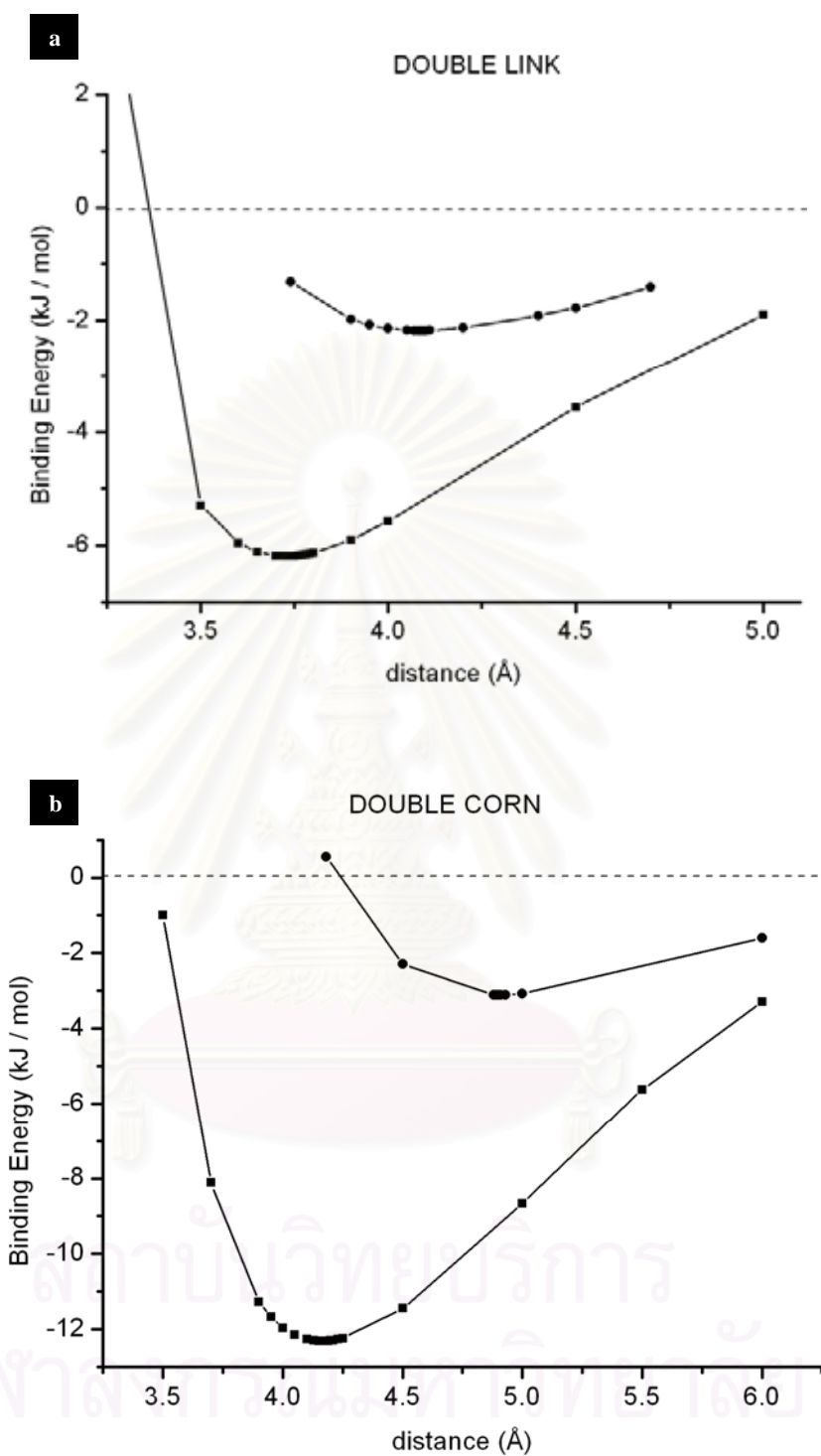


Figure 4.4 ONIOM binding energies (●) with BSSE and (■) without BSSE corrections for the CH₄/MOF-5 complexes where CH₄ was located in the H-in configuration (a) for the DOUBLE linker (LINK) and (b) for the DOUBLE corner (CORN) calculations, the distances were measured from the C atom of CH₄ to C_g and O₁, respectively (see Figure 3.2a).

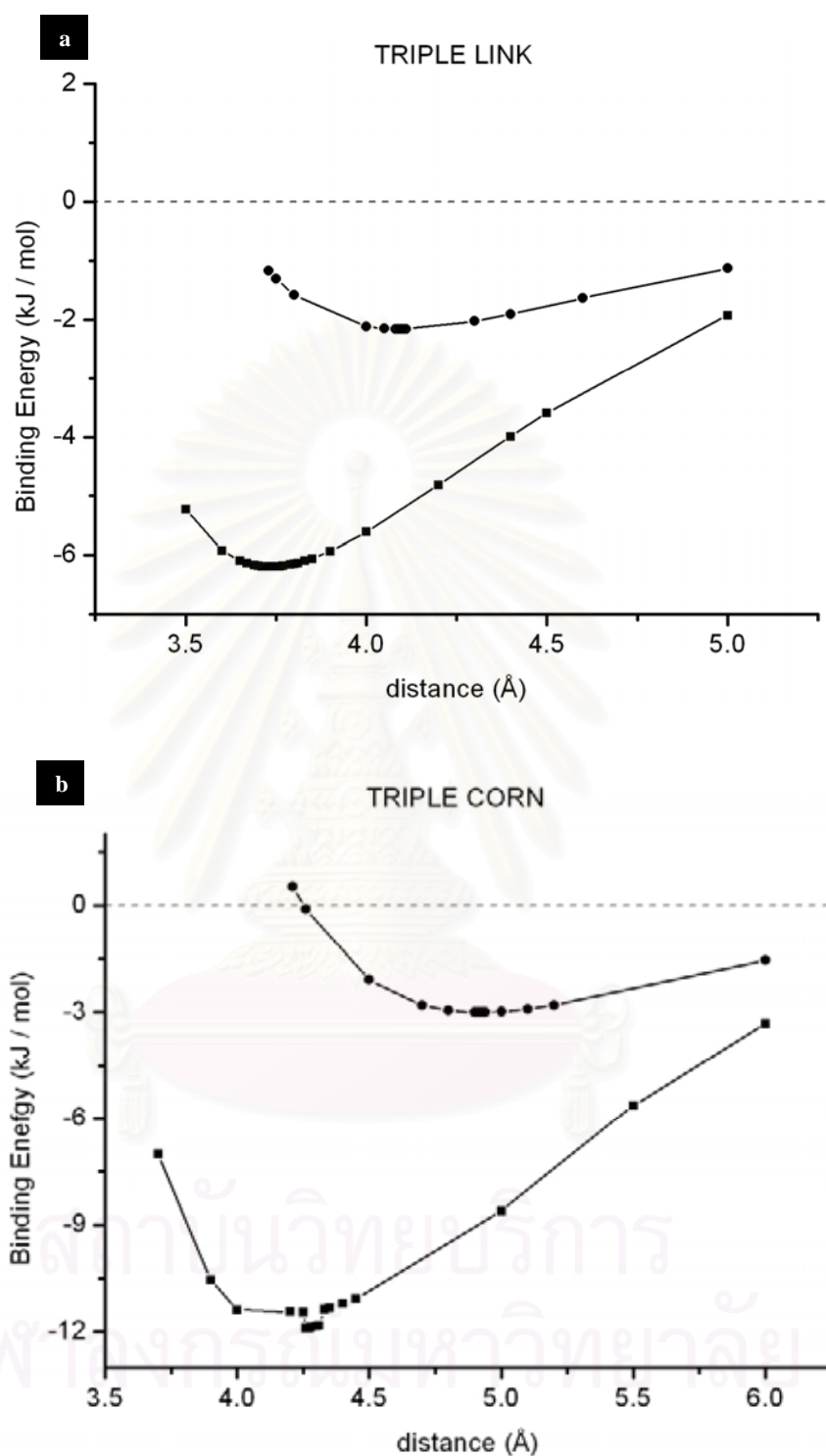


Figure 4.5 ONIOM binding energies (●) with BSSE and (■) without BSSE corrections for the CH₄/MOF-5 complexes where CH₄ was located in the H-in configuration (a) for the TRIPLE linker (LINK) and (b) for the TRIPLE corner (CORN) calculations, the distances were measured from the C atom of CH₄ to C_g and O₁, respectively (see Figure 3.2a).

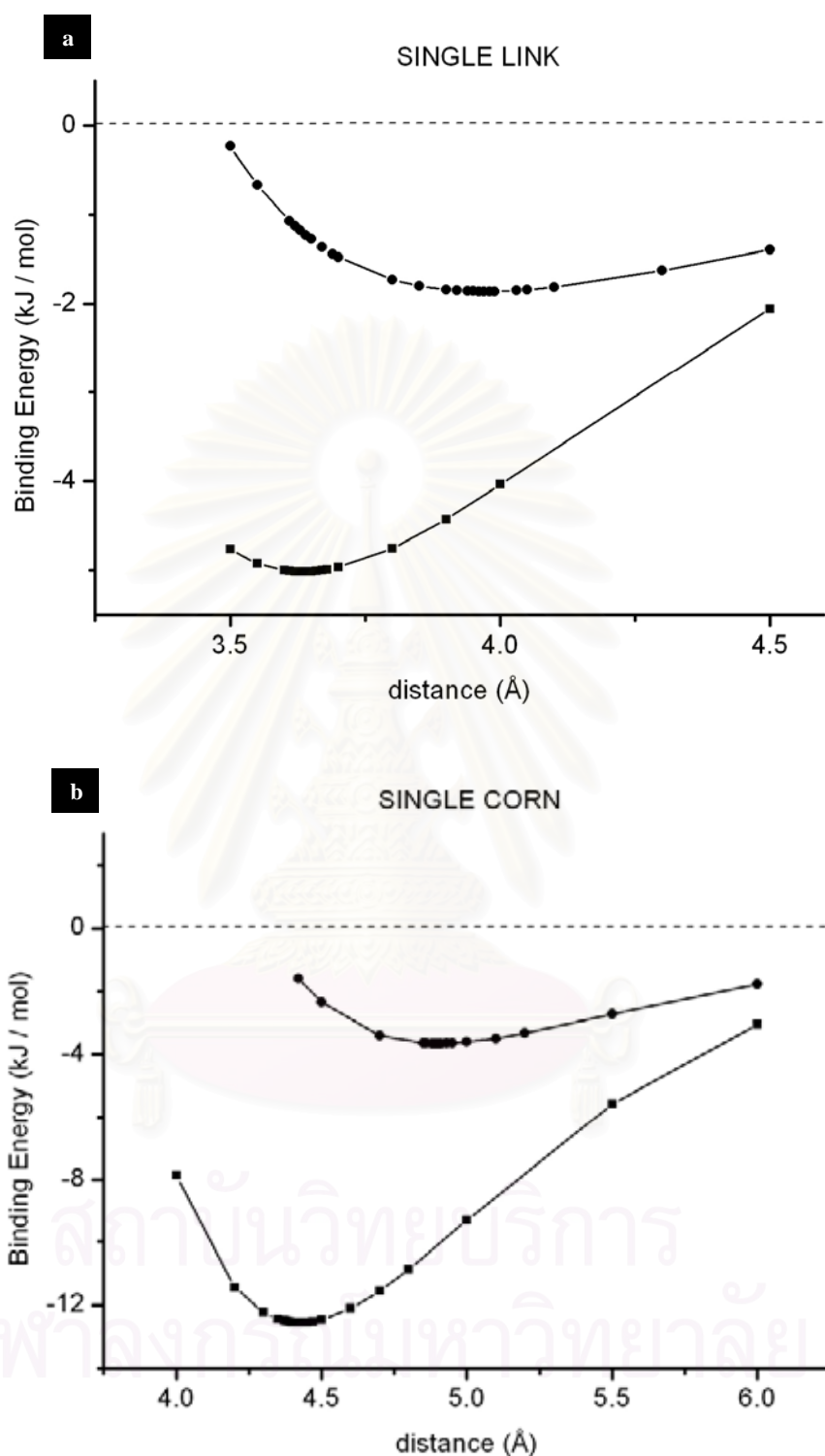


Figure 4.6 ONIOM binding energies (●) with BSSE and (■) without BSSE corrections for the CH₄/MOF-5 complexes where CH₄ was located in the H-out configuration (a) for the SINGLE linker (LINK) and (b) for the SINGLE corner (CORN) calculations, the distances were measured from the C atom of CH₄ to C_g and O₁, respectively (see Figure 3.2a).

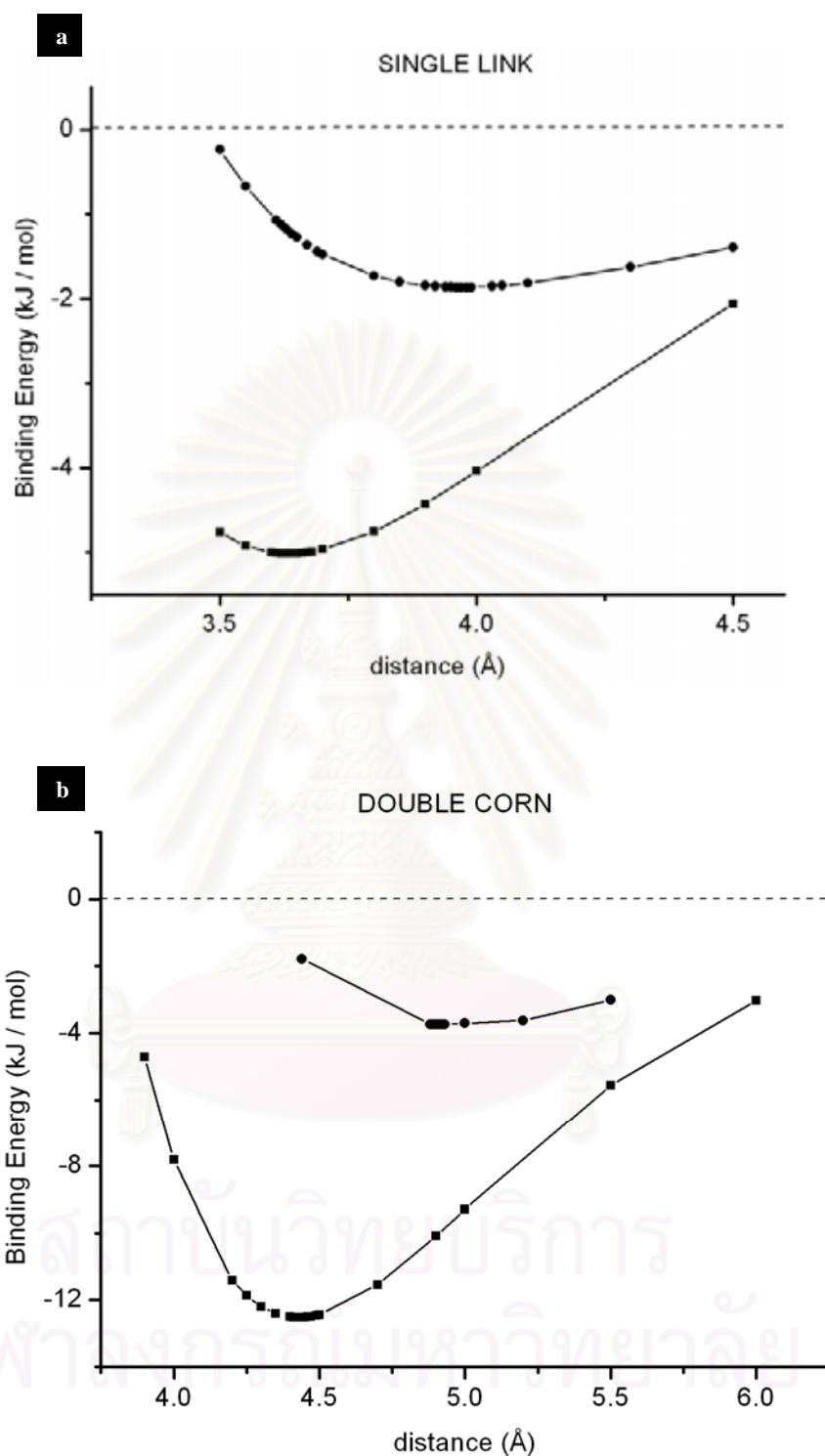


Figure 4.7 ONIOM binding energies (●) with BSSE and (■) without BSSE corrections for the CH₄/MOF-5 complexes where CH₄ was located in the H-out configuration (a) for the DOUBLE linker (LINK) and (b) for the DOUBLE corner (CORN) calculations, the distances were measured from the C atom of CH₄ to C_g and O₁, respectively (see Figure 3.2a).

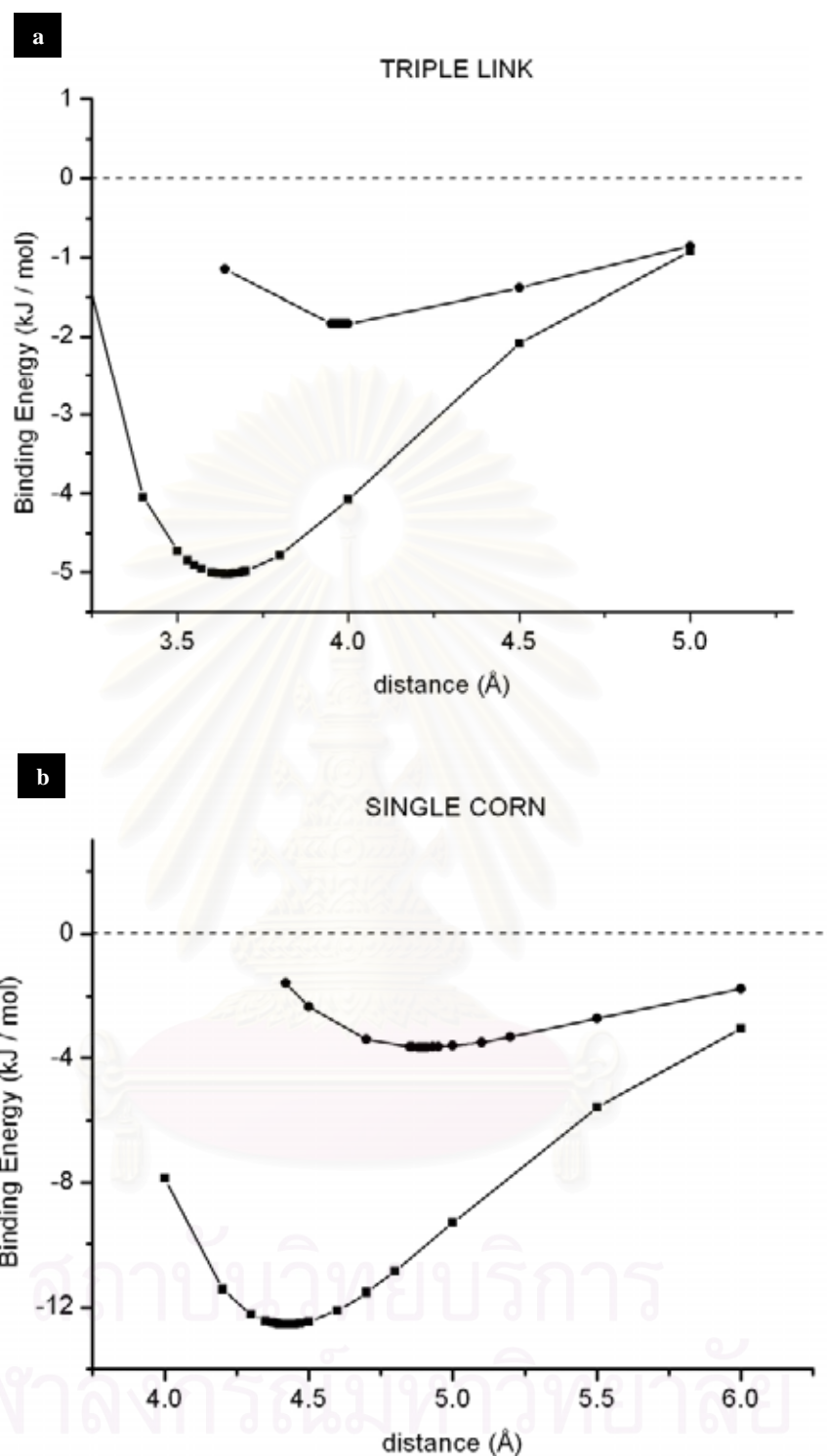


Figure 4.8 ONIOM binding energies (●) with BSSE and (■) without BSSE corrections for the CH₄/MOF-5 complexes where CH₄ was located in the H-out configuration (a) for the DOUBLE linker (LINK) and (b) for the DOUBLE corner (CORN) calculations, the distances were measured from the C atom of CH₄ to C_g and O₁, respectively (see Figure 3.2a).

It can be seen from Table 4.3 and 4.4 that size of the fragment does not effect significantly to the energy and structure of binding at both corner and linker sites. This is in contrast to what observed for the CO₂-MOF where size of the fragment plays strong role on those properties, especially at the corner of the unit cell[50]. The optimal structure of methane-lattice complexes at the linker site of the biggest fragment (TRIPLE) gives the energy with BSSE corrections of -1.83 kJ/mol in the H-out orientation with the distance Cg-C of 3.98 Å. Such weak interaction is known to be due to the fact that the interaction with the benzene ring (see Figure 3.2a) of the linker unit is dominated by the dispersion forces. This is not the case for the corner where the interaction is influenced by electronic forces due to the Zn cluster unit. Therefore, the corresponding binding energy and the O₁-C distance are -3.80 kJ/mol and 4.90 Å, respectively.

The Figures 4.3-4.8 as well as the data in Tables 4.3 and 4.4 show that the BSSE leads to dramatic changes of the calculated results. Distance to the minimum changes from 3.73 Å to 4.08 Å for the SINGLE LINK cluster H-in orientation and from 4.19 Å to 4.92 Å for the SINGLE CORN cluster H-in orientation. The corresponding interaction energies for the linker and corner were observed to change by ~3 kJ/mol and ~9 kJ/mol, respectively, shifted to weaker interactions. The observed results indicate obviously that the investigated systems requires BSSE corrections. Since the two-body method is applied in all molecular adsorption cases and this correction should be included in all energy values.

4.4 Binding Energy of CH₄ in IRMOF-6 and IRMOF-14

In these complexes, the method of ONIOM (MP2/6-31G** : HF/6-31G**) with BSSE was again used. The lattices SINGLE, DOUBLE and TRIPLE were optimized as in the case of IRMOF-1. The structures and energies of methane-IRMOF-6 complexes are summarized in Table 4.5 and 4.6. At the linker, the most favourable orientation of the CH₄ molecule is H-in with the Cg-C distance and the corresponding energy of 4.04 Å and -2.89 kJ/mol, respectively.

The same as that found for IRMOF-1, sizes of the fragment are not influential to the adsorption energy. The adsorption energies at the corner site are -2.97 and -3.42 kJ/mol for the SINGLE cluster in H-in and H-out orientations, respectively. Increase of the fragment size to DOUBLE and TRIPLE models increases the overall adsorption energies in the range of 0.3-0.15 kJ/mol. The binding of CH₄ at the corner of all IRMOF-6 models show the same trend as those observed from the IRMOF-1 system in terms of both structures and energies.

Table 4.5 ONIOM binding energies with BSSE corrections and the corresponding distances between IRMOF-6 linker in the three cluster models (SINGLE, DOUBLE and TRIPLE) and CH₄ molecule.

Model		Distance Cg-C (Å)	Binding energy (kJ/mol)
IRMOF-6	CH ₄		
SINGLE	H-in	4.06	-2.85
	H-out	3.89	-2.50
DOUBLE			
Model I	H-in	4.02	-2.80
	H-out	3.88	-2.52
Model II	H-in	4.02	-2.81
	H-out	3.89	-2.63
TRIPLE			
Model I	H-in	4.04	-2.89
	H-out	3.87	-2.63
Model II	H-in	4.06	-2.87
	H-out	3.84	-2.58

Table 4.6 ONIOM binding energies with BSSE corrections and the corresponding distances between IRMOF-6 corner in the three cluster models (SINGLE, DOUBLE and TRIPLE) and CH₄ molecule.

Model		Distance O ₁ -C (Å)	Binding energy (kJ/mol)
IRMOF-6	CH ₄		
SINGLE	H-in	5.08	-2.97
	H-out	4.90	-3.42
DOUBLE			
Model I	H-in	5.06	-3.04
	H-out	4.95	-3.50
Model II	H-in	5.09	-3.08
	H-out	4.93	-3.47
TRIPLE			
Model I	H-in	5.03	-3.12
	H-out	4.93	-3.53
Model II	H-in	5.07	-3.15
	H-out	4.91	-3.54

Table 4.7 ONIOM binding energies and the corresponding distance with the BSSE corrections for the CH₄-IRMOF-14 complex.

A: At the IRMOF-14 linker

Model		Distance Cg-C (Å)	Binding energy (kJ/mol)
IRMOF-14	CH ₄		
SINGLE			
Model I	H-in	3.96	-3.67
	H-out	3.77	-3.53
Model II	H-in	3.93	-3.63
	H-out	3.73	-3.58
DOUBLE			
Model I	H-in	3.96	-3.65
	H-out	3.74	-3.54
Model II	H-in	3.96	-3.71
	H-out	3.72	-3.50
Model III	H-in	3.98	-3.77
	H-out	3.78	-3.49
TRIPLE			
Model I	H-in	3.96	-3.75
	H-out	3.77	-3.47
Model II	H-in	3.95	-3.71
	H-out	3.73	-3.55
Model III	H-in	3.97	-3.73
	H-out	3.77	-3.58

B: At the IRMOF-14 corner

Model		Distance O ₁ -C (Å)	Binding energy (kJ/mol)
IRMOF-14	CH ₄		
SINGLE	H-in	4.96	-3.06
	H-out	5.05	-3.50
DOUBLE	H-in	4.97	-3.02
	H-out	5.07	-3.14
TRIPLE	H-in	4.93	-3.07
	H-out	5.04	-3.36

Table 4.7 shows the calculation energies and structures of the CH₄ in the IRMOF-14 complexes. The distances and configuration used were shown in Figure 3.10. The optimal structure of methane-IRMOF-14 complex is H-in orientation at the linker site with the binding energy of -3.75 kJ/mol and the corresponding Cg-C distance of 3.96 Å (TRIPLE model). The conjugation linker of bigger size does not affect the adsorption energies of the system. The interaction of the IRMOF-14 corner is similar to that in the IRMOF-1 and IRMOF-6.

CHAPTER V

CONCLUSIONS

Natural gas mainly consisting of methane is a valuable alternative to be more conventional fuels, however, its very low intrinsic density constitutes a major disadvantage in practical application. To find a new desirable material for methane storage, specific accessible area, free volume, and low density of framework should be considered. Thus, the comparison of methane adsorption in various IRMOFs was investigated in this work.

To validate reliability of the methods and the basis sets used, the calculations were firstly examined on various systems of benzene and its derivatives with methane molecule. The obtained results suggest that the binding interactions of the system are obviously weak, therefore, the DFT and HF calculations are not suitable. By contrast, MP2 theory should give accurate results in this case. It was, then, applied to investigate interaction energy for all systems. Large basis sets are necessary to provide the required accuracy for investigated systems.

To describe the adsorption energy of methane within IRMOFs, the interactions between CH₄ molecule and several IRMOFs in three cluster sizes, SINGLE, DOUBLE and TRIPLE, are studied. The ONIOM (MP2/6-31G** : HF/6-31G**) method was carried out to obtain the optimal binding site, orientation as well as the binding energy of the complexes. CH₄ molecule with the configurations H-in and H-out was assigned to the linker (LINK) and corner (CORN) domains. The basis set superposition error corrections was also found to effect the calculated results significantly, both minimal distance and binding energy. The cluster size of SINGLE is sufficiently representative of the interactions at both linker and corner domains of the IRMOFs series with CH₄ molecules.

REFERENCES

- [1] Eddaoudi, M., KiM, J., Rosi, N., Vodak, D., O'Keeffe, M., and Yaghi, O.M., "Systematic Design of Pore Size and Functionality in Isoreticular MOFs and Their Application in Methane Storage", *Science*, **2002**, 295, 469-472.
- [2] Ward, M.D., "Molecular Fuel Tanks", *Science*, **2003**, 300, 1104-1105.
- [3] Eddaoudi, M., O'Keeffe, M. and Yaghi, O.M., "Design and Synthesis of an Exceptionally Stable and Highly Porous Metal-organic framework", *Nature*, **1999**, 402, 276-279.
- [4] Yaghi, O.M., O'Keeffe, M., Ockwig N.W., Chae, H.K., Eddaoudi, M., and KiM, J., "Reticular synthesis and the design of new materials", *Nature*, **2003**, 423, 705-714.
- [5] Celzard, A., Fierro, V., "Preparing a Suitable Material Designed for Methane Storage: A Comprehensive Report", *Energy Fuels*, **2005**, 19, 573-583.
- [6] Bhatia, S.K., Myers, A.L., "Optimum Conditions for Adsorptive Storage", *Langmuir*, **2006**, 22, 1688-1700.
- [7] Yaghi, O.M. and Rowsell, L.C., "Metal–Organic Frameworks: A New Class of Porous Materials", *Microporous Mesoporous Mater*, **2004**, 73, 3-14.
- [8] Reineke, T. M., Eddaoudi, M., O'Keeffe, M., and Yaghi, O. M., "A Microporous Lanthanide-Organic Framework", *Angew, Chem. Int. Edn Engl*, **1999**, 38, 2590-2594.
- [9] Reineke, T., Eddaoudi, M., Fehr, M., Kelley, D., and Yaghi, O. M., "From Condensed Lanthanide Coordination Solids to Microporous Frameworks Having Accessible Metal Sites", *J. Am. Chem. Soc.*, **1999**, 121, 1651-1657.

- [10] Eddaoudi, M., Li, H., and Yaghi, O. M., “Highly Porous And Stable Metal-Organic Frameworks: Structure Design and Sorption Properties”, *J. Am. Chem. Soc.*, **2000**, 122, 1391-1397.
- [11] Noro, S., Kitagawa, S., Kondo, M., and Seki, K., “A New, Methane Adsorbent, Porous Coordination Polymer [$\{\text{CuSiF}_6(4,4\text{-bipyridine})_2\}_n$]”, *Angew. Chem. Int. Ed.*, **2000**, 39, 2081-2084.
- [12] Gregory, J.H., Cameron J.K., Boujemaa M., Keith S.M., and John D.C., “Guest-Dependent Spin Crossover in a Nanoporous Molecular Framework Material”, *Chem. Mater.*, **2000**, 12, 1762-1765.
- [13] Rowsell L.C., Spencer, E.C., Eckert, E., Howard, A.K., and Yaghi, O.M., “Gas Adsorption Sites in a Large-Pore Metal-Organic Framework”, *Science*, **2003**, 300, 1350-1354.
- [14] Ma, S., Sun, D., Wang, X.S., and Zhou, H.C., “A Mesh-Adjustable Molecular Sieve for General Use in Gas Separation”, *Angew. Chem., Int. Ed.*, **2007**, 46, 2458-2462.
- [15] Chen, B., Liang, C., Yang, J., Contreras, D.S., Clancy, Y.L., Lobkovsky, E.B., Yaghi, O. M., and Dai, S. “A Microporous Metal-Organic Framework for Gas-Chromatographic Separation of Alkanes”, *Angew. Chem. Int. Ed.*, **2006**, 45, 1390-1393.
- [16] Lee, J., Li, J., and Jagiello, J., “Gas sorption properties of microporous metal Organic Frameworks”, *J. Solid State Chem.*, **2005**, 178, 2527-2532.
- [17] Lin, X., Jia, J., Zhao, X., Thomas, K. M., Blake, A.J., Walker, G.S., Champness, N.R., Hubberstey, P., Schröder, M., “High H₂ Adsorption by Coordination-Framework Materials”, *Angew. Chem., Int. E.*, **2006**, 45, 7358-7364.

- [18] Halder, G.J., Kepert, C.J., Moubaraki, B., Murray, K. S., Cashion, J.D.,
“Molecular Framework Material Guest-Dependent Spin Crossover in a
Nanoporous”, *Science*, **2002**, 298, 1762-1765.
- [19] Cheng, X.N., Zhang, W.X., Lin, Y.Y., Zheng, Y.Z., and Chen, X.M.,
“A Dynamic Porous Magnet Exhibiting Reversible Guest-Induced
Magnetic Behavior Modulation”, *Adv. Mater.*, **2007**, 19, 1494-1498.
- [20] Alvaro, M., Carbonell, E., Ferrer, B., Llabrés I., Xamena, F.X., and Garcia, H.,
“Semiconductor Behavior of a Metal-Organic Framework (MOF)”,
Chem. Eur. J., **2007**, 13, 5106-5112.
- [21] Rancesc X., Llabrés I.X., Alberto A., Avelino C., and Hermenegildo G.,
“MOFs as catalysts: Activity, reusability and shape-selectivity of a
Pd-containing MOF”, *J. Catal.*, **2007**, 250, 294-298.
- [22] Hoskins, B.F., and Robson, R., “Infinite Polymeric Frameworks Consisting of
Three Dimensionally Linked Rod-Like Segments”, *J. Am. Chem. Soc.*,
1989, 111, 5962-5964.
- [23] Hoskins, B.F., and Robson, R., “Design and construction of a new class of
scaffolding-like materials comprising infinite polymeric frameworks of
3D-linked molecular rods. A reappraisal of the zinc cyanide and cadmium
cyanide structures and the synthesis and structure of the diamond-related
frameworks $[N(CH_3)_4][CuIZnII(CN)_4]$ and
 $CuI[4,4',4'',4''']tetracyanotetraphenylmethane]BF_4 \cdot xC_6H_5NO_2$ ”,
J. Am. Chem. Soc., **1990**, 112, 1546-1554.

- [24] Abrahams, B.F., Hoskins, B.F., Liu, J., and Robson, R., "The archetype for a new class of simple extended 3D honeycomb frameworks. The synthesis and x-ray crystal structures of $\text{Cd}(\text{CN})_{5/3}(\text{OH})_{1/3} \cdot 1/3(\text{C}_6\text{H}_{12}\text{N}_4)$, $\text{Cd}(\text{CN})_{2.1/3}(\text{C}_6\text{H}_{12}\text{N}_4)$, and $\text{Cd}(\text{Cn})_{2.2/3}\text{H}_2\text{O} \cdot \text{tBuOH}$ ($\text{C}_6\text{H}_{12}\text{N}_4$ = hexamethylenetetramine) revealing two topologically equivalent but geometrically different frameworks", *J. Am. Chem. Soc.*, **1991**, 113, 3045-3051.
- [25] Abrahams, B.F., Hoskins, B.F., Liu, J., and Robson, R., "A New type of Infinite 3D Polymeric Network Containing 4-Connected, Peripherally-Linked Metalloporphyrin Building Blocks" *J. Am. Chem. Soc.*, **1991**, 113, 1606-1607.
- [26] Moulton, B., and Zaworotko, M. J., "From Molecules to Crystal Engineering: Supramolecular Isomerism and Polymorphism in Network Solids", *J. Chem. Rev.*, 2001, 101(6), 1629-1658.
- [27] Eddaoudi, M., Moler, D.B., Li, H., Chen, B., Reineke, T.M., O'Keeffe, M., and Yaghi, O. M., "Modular Chemistry: Secondary Building Units as a Basis for the Design of Highly Porous and Robust Metal-Organic Carboxylate Frameworks", *Acc. Chem. Res.*, **2001**, 34(4), 319-330.
- [28] Kitagawa, S., Kitaura, R., and Noro, S.I., "Functional Porous Coordination Polymers", *Angew. Chem., Int. Ed.*, **2004**, 43, 2334-2375.
- [29] Wells, A. F. *Structural Inorganic Chemistry*, 5th ed.; Oxford University Press: Oxford, 1984.
- [30] Yaghi, O. M., Davis, C. E., Li, G., and Li, H., "Selective Guest Binding by Tailored Channels in a 3-D Porous Zinc(II)-Benzenetricarboxylate Network", *J. Am. Chem. Soc.*, **1997**, 119(12), 2861-2868.

- [31] Seo, J.S., Whang, D., Lee, H., Jun, S.I., Oh, J., and Kim, K., "A Homochiral Metal-Organic Porous Material for Enantioselective Separation and Catalysis", *Nature*, **2000**, 404, 982-986.
- [32] Rosi, N. L., Eckert, J., Eddaoudi, M., Vodak, D. T., Kim, J., O'Keeffe, M., and Yaghi, O.M., "Hydrogen Storage in Microporous Metal-Organic Frameworks", *Science*, **2003**, 300, 1127-1129.
- [33] Sagara, T., Klassen, J., and Ganz E., "Computational Study of Hydrogen Binding by Metal-Organic Framework-5", *J. Chem. Phys.*, **2004**, 121, 12543-12547.
- [34] Bordiga, *et al.*, "Interaction of Hydrogen with MOF-5", *J. Phys. Chem. B*, **2005**, 109, 18237-18242.
- [35] Buda, C., and Dunietz, B.D., "Hydrogen Physisorption on the Organic Linker in Metal Organic Frameworks: Ab Initio", 2006, 110, 10479-10484.
- [36] Levine, N. I. Quantum Chemistry. 5th ed. University of New York: Prentice Hall, 2000.
- [37] Møller C., Plesset M.S., "Note on Approximation Treatment for Many-Electron System", *Phys. Rev.*, **1934**, 46, 618-622.
- [38] Leininger M.L., Allen W.D., Schaefer H.F., and Sherrill C.D., "Is Moller-Plesset Perturbation Theory a Convergent *ab initio* Method", *J. Chem. Phys.*, 2000, 112(21), 9213-9222.
- [39] Lewar, E. Computational Chemistry. United States of America:Kluwer Academic Publishers, 2003.

- [40] Jensen, F. Introduction to Computational Chemistry. Odense University:John Wiley & Sons, 1999.
- [41] Humbel, S., Sieber, S., and Morokuma, K., "The IMOMO Method: Integration of Different Levels of Molecular Orbital Approximations for Geometry Optimization of Large Systems: Test for N-butane Conformation and SN2 Reaction: RC_1+Cl ", *J. Chem. Phys.*, **1996**, 105, 1959-1967.
- [42] Svensson, M., et al., ONIOM: A Multilayered Integrated MO+MM Method for Geometry Optimizations and Single Point Energy Predictions. A Test for Diels-Alder Reactions and $Pt(P(t-Bu)_3)_2 + H_2$ Oxidative Addition. *J. Phys. Chem.*, **1996**, 105, 19357-19363.
- [43] Maseras, F., Hybrid Quantum Mechanics/Molecular Mechanics Methods in Transition Metal Chemistry. *Top. Organomet. Chem.*, **1999**, 4, 165-191.
- [44] Vreven, T. and Morokuma, K., On the Application of the IMOMO (Integrated Molecular Orbital + Molecular Orbital) Method. *J. Comp. Chem.*, **2000**, 21, 1419-1432.
- [45] Morokuma, K., ONIOM and Its Applications to Material Chemistry and Catalyses. *Bull. Kor. Chem. Soc.*, **2003**, 24, 797-801.
- [46] Vreven, T., et al., Combining Quantum Mechanics Methods with Molecular Mechanics Methods in ONIOM. *J. Chem. Theo. Comp.*, **2006**, 2, 815-826.
- [47] Frisch, M. J., et al. *Gaussian 03*, Revision C.02; Wallingford CT: Gaussian, Inc., 2004.
- [48] Mourik, T., "On the relative stability of two noradrenaline conformers", *Chem. Phys. Lett.*, **2005**, 414, 364-368.

- [49] Huang, B.L., McGaughey, A.J.H, and Kaviany, M., “Thermal conductivity of metal-organic framework 5 (MOF-5): Part I. Molecular dynamics simulations”, . *J. Heat Mass Transfer.*, **2007**, 50, 393-404.
- [50] Pianwanit et *al.*, “The optimal binding sites of CH₄ and CO₂ molecules on the metal-organic framework MOF-5: ONIOM calculations” , *Chemical. Physics.*, **Accepted**.



สถาบันวิทยบริการ
จุฬาลงกรณ์มหาวิทยาลัย



APPENDICES

สถาบันวิทยบริการ
จุฬาลงกรณ์มหาวิทยาลัย



The optimal binding sites of CH₄ and CO₂ molecules on the metal-organic framework MOF-5: ONIOM calculations

Atchara Pianwanit^a, Chinapong Kritayakornupong^b, Arthit Vongachariya^a,
Nattaya Selphusit^c, Tanawut Ploymeerusmee^c, Tawun Remsungnen^d, Duangamol Nuntasri^a,
Siegfried Fritzsche^e, Supot Hannongbua^{a,*}

^a Department of Chemistry, Faculty of Science, Chulalongkorn University, Bangkok 10330, Thailand

^b Department of Chemistry, Faculty of Science, King Mongkut's University of Technology Thonburi, Bangkok 10140, Thailand

^c Petrochemical and Polymer Science Program, Faculty of Science, Chulalongkorn University, Bangkok 10330, Thailand

^d Department of Mathematics, Faculty of Science, Khon Kaen University, Khon Kaen 40002, Thailand

^e Institute for Theoretical Physics, University Leipzig, Postfach 100920, D-04009, Leipzig, Germany

Received 10 October 2007; accepted 20 February 2008

Abstract

Optimal binding sites and its corresponding binding energies between MOF-5 clusters and small guest molecules, CH₄ and CO₂, were investigated using the ONIOM method with different levels of quantum chemical calculations. The clusters were validated using three different sizes of the MOF-5 clusters, SINGLE, DOUBLE and TRIPLE consisting of (Zn₄O)₂(COOCH₃)₁₀(COO)₂C₆H₄, (Zn₄O)₃-(COOCH₃)₁₄(COO)₄(C₆H₄)₂ and (Zn₄O)₄(COOCH₃)₁₈(COO)₆(C₆H₄)₃ units, respectively. Guest molecules were assigned to lie in the configurations parallel (||) and perpendicular (⊥) to linker (LINK) and corner (CORN) domains of the clusters. The ONIOM(MP2/6-31G**:*HF*/6-31G**) with the corrections due to the basis set superposition errors was found to be the optimal choice for the investigation of these systems. Strong effects of cluster size were found for the CO₂/MOF-5 complexes, i.e., the SINGLE cluster is sufficient to represent interactions with CH₄, but the interaction with CO₂ requires the TRIPLE model. The optimal binding sites of guest molecules as well as their orientations in the cavity of the MOF-5 are CORN⊥ for both CH₄ and CO₂ with the corresponding binding energies of −3.64 and −9.27 kJ/mol, respectively.

© 2008 Elsevier B.V. All rights reserved.

Keywords: Metal-organic frameworks; MOF-5; Quantum calculations; ONIOM; Methane; Carbon dioxide

1. Introduction

Metal-organic frameworks (MOFs) are a new class of porous materials which becomes a promising target for gas adsorption, storage and separation [1–3]. Attempts to use alternative fuels such as hydrogen and methane instead of the conventional fuels such as gasoline and diesel have raised the studies of storage applications for such MOFs [4]. Moreover, MOFs have been utilized for separation

and purification of gas mixtures (H₂/CO₂/CH₄). Yaghi and his group introduced the first stable crystal structure of the MOF-5 and generated series of the iso-reticular metal-organic frameworks (IRMOFs) [5–8]. The structure of the IRMOFs composes of basic zinc acetate unit (Zn₄O(CO₂)₆) and linking units (LINK) which are rigid linear dicarboxylate groups. Both units are strongly bonded providing a well-defined structure in which different linking units are possible. In view of an advantage of the modification of such linking units, the MOFs are considered to be the most powerful targets for new storage media in the near future. The understanding of guest–host interactions as well as related properties at molecular level is the key of

* Corresponding author. Tel./fax: +66 2218 7603.

E-mail address: Supot.H@Chula.ac.th (S. Hannongbua).

success to design and discover new class of materials and becomes the main goal of this study.

Some attempts have been made using quantum chemical calculations to study H₂–MOF-5 interaction. Sagara et al. [9,10] calculated the binding energy based on the second-order Møller–Plesset perturbation theory (MP2) with some models of linker and corner sites. The results show that the binding energy at the corner site (~6–7 kJ/mol) is a little bit stronger than once at the linker site (~4–5 kJ/mol). In addition, the investigation of Lee et al. [11] using density functional theory (DFT) shows that the interaction between the simple benzene ring with H₂ is significantly changed when the benzene ring has been incorporated into the framework of MOF-5. Moreover, molecular dynamics simulations have been performed for predicting the adsorption sites of the H₂ [12,13] on the MOF-5 structure. The results again, indicate that hydrogen adsorbs rather strongly at the sites near the zinc acetate cluster and less strongly at the sites near the 1,4-benzenedicarboxylate linker. Yang and Zhong [14] also found that the selectivity of gas absorption is almost pressure-independent. These above results clearly show that the calculated results depend significantly on method and model employed.

To our knowledge, no experimental results are available on the position of preferential CH₄ and CO₂ sites, only neutron spectroscopic techniques proposes at least two different adsorption sites with considerably strong interaction [1]. In this study, different levels of the ONIOM method were applied to investigate the interaction between MOF-5 and small guest molecules, CH₄ and CO₂, aimed to understand their preferential binding site in the cavity of the MOF-5. The investigations were also extended to seek

for the optimal method used, optimal cluster size of the MOF and the effect of the unbalance of the basis set.

2. Computational details

2.1. Initial structure of the MOF-5

A column consisting of two corners connected by a linker, (Zn₄O)₂(COOCH₃)₁₀(COO)₂C₆H₄, was generated (Fig. 1a). It was, then, used to build up the whole MOF-5 unit cell (Fig. 1b). Aimed to get reliable geometries of the MOF-5 relative to experimental data [5], the two fragments were fully optimized using various quantum mechanical methods (semi-empirical, HF, DFT) and basis sets. All optimization and energy calculation were performed using Gaussian03 [15].

2.2. The models

Seeking for an optimal compromise between fragment size vs. the required computer time, different quantum mechanical methods and fragment sizes were examined. The MOF-5 was represented by the three models shown in Fig. 2a. The fragments consisting of 1, 2 and 3 columns were named, for simplicity, as SINGLE, DOUBLE and TRIPLE, respectively.

For interaction with the linker (LINK), guest molecules were generated to move along the vector perpendicular to the molecular plane of the benzene ring at the C_g (see Fig. 1a for definition). For the DOUBLE and TRIPLE models, calculations were carried out only for one wing of the fragments. Here, two possible orientations of guest

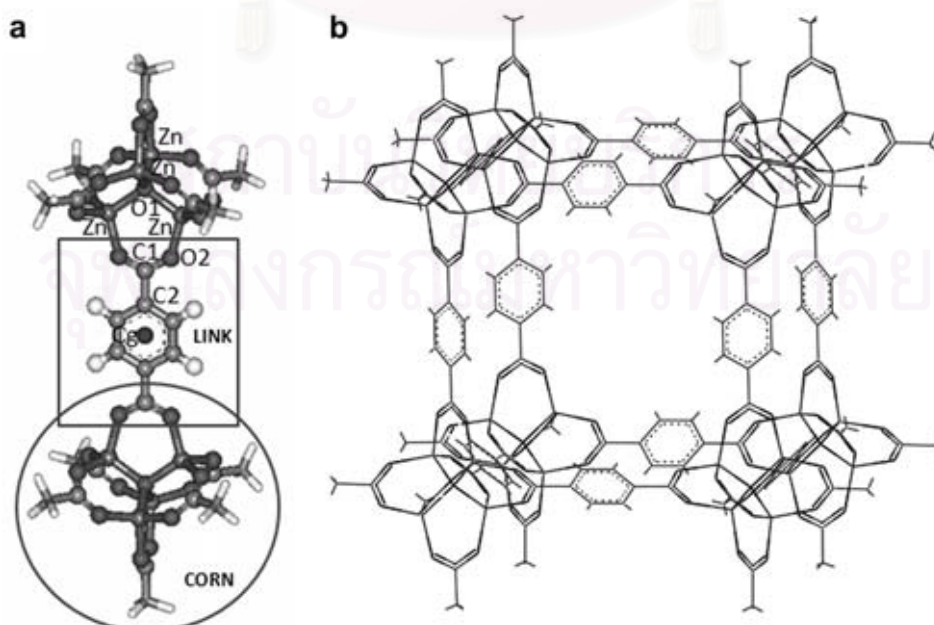


Fig. 1. (a) A single fragment of the MOF-5 consisting of two corners and one linker and (b) the whole MOF-5 unit cell which were generated as initial structures to be used in this study where C_g denotes center of mass of the benzene ring.

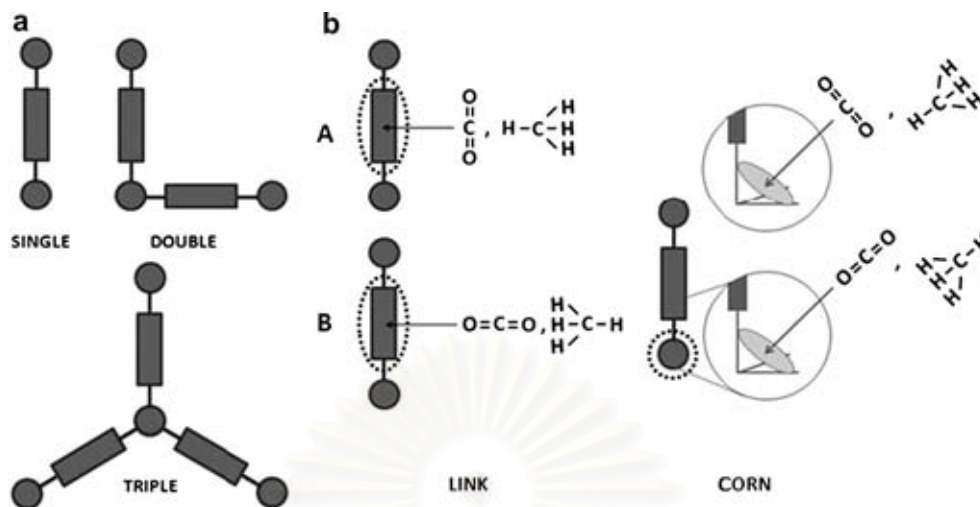


Fig. 2. Representation of the calculated models where rectangular and filled-circle represent linker and corner, respectively, and dot-circle denotes the model part for which high level of accuracy in the ONIOM calculation was applied. (a) Models SINGLE, DOUBLE and TRIPLE represent the MOF fragments containing one, two and three units as oriented, respectively, where one unit of the model is composed of two corners connected by a linker (Fig. 1a). (b) Orientation of guest molecules in parallel (A) and perpendicular (B) to the binding site (linker or corner).

molecules were taken into account, parallel (\parallel) and perpendicular (\perp) to the MOF fragments as shown in Fig. 2b. Precisely, \parallel and \perp for CH₄ means that it points one H atom forward and backward the MOF fragment, respectively. For the MOF corner (CORN), guest molecules, also in the two configurations, were generated to move along the vector pointing to O1 (see Fig. 1a). Note that the vector denotes the C₃-symmetry axis of the three O1–Zn bonds of the MOF corner.

2.3. ONIOM calculations including BSSE

Referred to the three SINGLE, DOUBLE and TRIPLE models defined in Section 2.2, the ONIOM interaction energy of each system, ΔE_{ONIOM} , is derived as

$$\Delta E_{\text{ONIOM}} = E_{(\text{real},\text{low})} + E_{(\text{model},\text{high})} - E_{(\text{model},\text{low})}, \quad (1)$$

where $E_{(\text{real},\text{low})}$ is the total energy of the real system using the low level method, while $E_{(\text{model},\text{high})}$ and $E_{(\text{model},\text{low})}$

Table 1

Selected bond distances and bond angles obtained from the geometry optimizations for the two clusters shown in Fig. 1 where the experimental data [5] and the other theoretical calculations [16,17] were also given for comparison (see Fig. 1 for atomic labels)

Method/basis set	Bond length (pm)				Bond angle (°)		
	Zn–O ₁	Zn–O ₂	O ₂ –C ₁	C ₁ –C ₂	O ₁ –Zn–O ₂	Zn–O ₂ –C ₁	O ₂ –C ₁ –C ₂
<i>(a) One column cluster (Fig. 1a)</i>							
AM1	205.5	212.4	128.5	148.5	110.1	134.2	119.0
PM3	195.1	205.3	127.6	150.7	112.4	131.2	118.2
HF/6-31G*	197.8	196.9	124.5	149.7	110.1	132.8	117.7
HF/6-31G**	197.8	196.9	124.5	149.7	110.1	132.8	117.7
B3LYP/6-31G*	195.4	195.0	127.0	149.6	111.2	131.1	117.2
B3LYP/6-31G**	195.3	195.1	127.0	149.6	111.1	131.2	117.2
B3LYP/6-311G**	196.1	195.7	126.4	149.6	109.7	131.1	117.3
B3LYP/6-311G** [16]	197.2	195.3	126.2	151.0	110.8	131.7	117.8
GULP [16]	212.6	195.7	127.2	138.8		134.5	120.3
MPW1PW91/6-31G**	194.0	194.0	126.4	149.1	111.2	131.0	117.2
<i>(b) One unit cell cluster (Fig. 1b)</i>							
AM1	205.4	212.1	128.5	148.5	110.2	134.2	119.0
PM3	195.1	205.4	127.5	150.7	112.1	130.7	117.6
B3LYP/6-31G**	195.3	194.8	127.0	149.6	111.4	131.1	117.3
AM1 [17]	205.5	212.4	128.4	148.5	110.1	134.2	119.0
PM3 [17]	195.1	205.6	127.5	150.7	112.1	130.6	117.5
Experimental data	193.6	194.1	125.2	149.8	111.1	132.3	118.1

denote the total energies of the model part calculated with high and low level methods, respectively. The method used for the high:low levels was represented by MP2/6-31G^{**}:HF/6-31G^{**}. The high accurate (model) MP2/6-31G^{**} part covers the compositions (C₆H₄) and the (Zn₄O(CO₂)₆) for the linker and corner domains, respectively, labeled as dot-circles in Fig. 2. The real parts were the whole SINGLE, DOUBLE and TRIPLE fragments shown in Fig. 2. Discrepancies due to an unbalance of the basis set used, known as basis set superposition error (BSSE) were examined and taken into account for all data points reported in this study.

3. Results and discussion

3.1. Geometries of the MOF-5

Starting from the two clusters, one column (Fig. 1a) and the whole unit cell (Fig. 1b) of the MOF-5, their intramolecular geometries (bond lengths and bond angles) were fully optimized using different methods and levels of accuracy. The results were summarized in Table 1.

Relative to experimental geometries [5], discrepancies were, as expected, found among the results obtained from different methods and basis sets used. The MPW1PW91/6-31G^{**} geometries for the one column cluster are in excellent agreement with the experimental data. Due to the fact that the MPW1PW91/6-31G^{**} is highly time consuming, it is practically impossible to apply it for the full unit cell cluster. Therefore, the optimal choice shifts to the next lower-accurate B3LYP/6-31G^{*} and B3LYP/6-31G^{**} meth-

ods. As shown in Table 1, no significant difference was found on the geometries of the clusters yielded from these two methods. However, the MP2/6-31G^{**} binding energy is slightly lower than that of MP2/6-31G^{*} (data not shown) although the time required is also slightly longer. Taking into account all the data mentioned earlier, the MP2/6-31G^{**}, with BSSE corrections, was chosen to represent the high accurate part of the ONIOM calculation.

Note that the results yielded from the two clusters, one column and one unit cell, are in good agreement. This indicates that size of the one column cluster is sufficient to represent intramolecular geometries of the MOF-5. In addition, our results, especially Zn–O1 and Zn–O2 distances, are closer to the experimental data [5] in comparison to those reported in Refs. [16,17].

3.2. Effect of an unbalance of the basis sets

Fig. 3 shows the ONIOM binding energies with and without BSSE corrections between CH₄ and the three clusters, SINGLE, DOUBLE and TRIPLE, of the MOF-5 (see Fig. 2a) where CH₄ points one H atom forward Cg or O1 and the distances are from C atom of CH₄ to Cg or O1 (see Fig. 1a) for linker (LINK||) or corner (CORN||) clusters, respectively.

It was surprisingly found from the plots that BSSE leads to dramatic changes of the calculated results. Distance to the minimum changes from 3.74 to 4.08 Å for the SINGLE LINK|| and from 4.19 to 4.92 Å for the SINGLE CORN|| clusters. The corresponding interaction energy differences for the linker and corner are ~3 and ~9 kJ/mol,

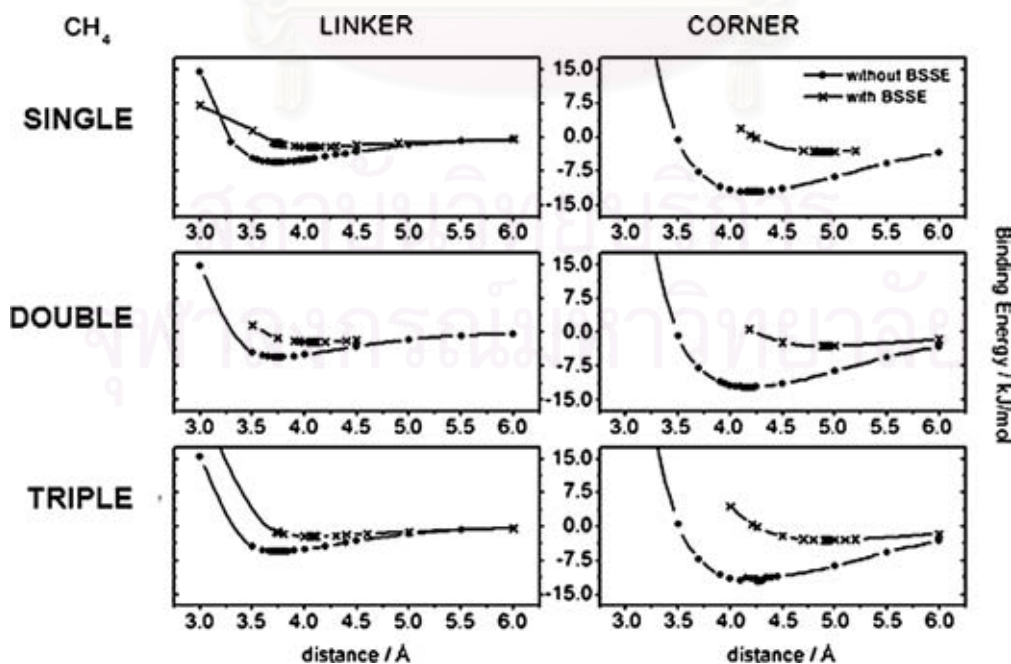


Fig. 3. ONIOM binding energies with and without BSSE corrections for the CH₄/MOF-5 complexes where CH₄ was located in the configuration pointing one H atom to the MOF-5 (||, see Fig. 2b) and the MOF-5 was represented by the SINGLE, DOUBLE and TRIPLE clusters (see Fig. 2a). For the linker (LINK) and corner (CORN) calculations, the distances were measured from the C atom of CH₄ to Cg and O1, respectively (see Fig. 1a).

respectively, shifted to weaker interactions. The observed results indicate obviously that the investigated systems requires BSSE corrections.

3.3. MOF-guest binding

ONIOM binding energy between MOF-5 in the three cluster models, SINGLE, DOUBLE and TRIPLE (Fig. 2a) and guest molecules in the two orientations, \parallel and \perp , (Fig. 2b) were calculated separately for the linker and corner parts and summarized in Table 2. The distances were measured from Cg (for linker) and O1 (for corner) to C atoms of CH₄ and CO₂. The BSSE corrections were applied in all data points.

Considering the binding energies at the same configuration of guest molecules (\parallel or \perp) at the linker part (Table 2a), no significant difference was found for the CH₄ complexes of different cluster sizes, SINGLE, DOUBLE and TRIPLE. However, the cluster size effect was slightly found for the CO₂ complexes, i.e., increasing of the MOF-5 cluster from SINGLE to TRIPLE leads to weaker binding energy (from -5.32 to -5.08 kJ/mol) for the \parallel whereas this change was opposite (from -1.61 to -2.02 kJ/mol) for the \perp configurations. For the effects of molecular orientation, the binding energy of the \parallel configuration for the CO₂/MOF-5 complexes is about three times more stable than that in the \perp configuration but only slightly different for the CH₄ complexes.

In contrast to what was observed for the linker, the calculated results at the MOF-5 corner (Table 2b) lead to the following two main conclusions: (i) CO₂ prefers to approach O1 (defined in Fig. 1b) at the corner of the MOF-5 in the \perp configuration, i.e., the binding energies

of the \parallel configuration of -4.94 , -3.55 and -2.25 kJ/mol are obviously less stable than those of the \perp configuration of -6.72 , -8.14 and -9.27 kJ/mol, respectively. A similar trend was, somehow, found for the CH₄ binding in which the interaction energy in the configuration where CH₄ points one H backward O1 is slightly lower than that when one H points forward O1. (ii) Effects of cluster size were found to be strong for the CO₂/MOF-5 complexes. As shown, an increasing of the cluster size from SINGLE to TRIPLE decreases the binding energy of the \parallel configuration from -4.94 to -2.25 kJ/mol. In contrast, this change leads to an increasing of the binding energy of the \perp configuration from -6.72 to -9.27 kJ/mol. The detected data let us conclude that for guest molecules of similar or bigger size than CO₂, the minimum cluster size to represent the MOF corner must contain at least three SINGLE MOF units (see Fig. 2a).

Taking into account all the data discussed above for both CH₄ and CO₂ molecules, interactions at the MOF's corner are stronger than those at the linker. This can be due to the fact that the interaction with the arene ring (see Fig. 1) of the linker unit is dominated by the dispersion forces. This is not the case for the MOF's corner where the interaction is influenced by electronic forces due to the (Zn₄O)₂(COOCH₃)₁₀ unit.

Note that the results show a certainly relevant trend of the interaction energies with CH₄ and CO₂ guest molecules. However, a higher level of quantum treatment is needed in order to provide an absolute value of the binding energies.

In summary, the optimal binding sites of guest molecules as well as their orientations in the cavity of the MOF-5 based on the binding energies shown in Table 2 are CORN \perp for both CH₄ and CO₂ complexes. In addition, the binding energies of the MOF-5 with the two guest molecules complexes are in the following order: CH₄: CORN \perp < CORN \parallel < LINK \parallel < LINK \perp and CO₂: CORN \perp < LINK \parallel < CORN \parallel < LINK \perp .

4. Conclusion

Quantum chemical calculations were carried out to find the optimal binding site and orientation as well as the binding energy of CH₄ and CO₂ molecules in the cavity of MOF-5. Guest molecules were assigned to lie in the configurations parallel (\parallel) and perpendicular (\perp) to linker (LINK) and corner (CORN) domains. The ONIOM (MP2/6-31G**.:HF/6-31G**) method was found to be a compromise between the accuracy and computer time required for the investigated system. Unbalance of the basis set used, known as basis set superposition errors, was found to effect the calculated results, both binding distance and energy, significantly. The cluster size of (Zn₄O)₂(COOCH₃)₁₀(COO)₂C₆H₄ is sufficient to represent interactions at both linker and corner domains of the MOF-5 with CH₄ molecules. However, for guest molecules of similar or bigger size than CO₂, the minimum cluster size to represent the MOF corner must contain at least one

Table 2

ONIOM binding energies with BSSE corrections and the corresponding distances between MOF-5 in the three cluster models (SINGLE, DOUBLE and TRIPLE in Fig. 2a) and guest molecules in the two orientations (\parallel and \perp in Fig. 2b) in which the distances were measured from Cg (for linker) and O1 (for corner) to C atoms of CH₄ and CO₂

Model		Distance Cg–C (Å)		Binding energy (kJ/mol)	
MOF-5	Guest	CH ₄	CO ₂	CH ₄	CO ₂
<i>(a) At the MOF-5 linker</i>					
SINGLE	\parallel	4.08	3.59	–2.15	–5.32
	\perp	3.97	4.64	–1.86	–1.61
DOUBLE	\parallel	4.09	3.58	–2.17	–5.16
	\perp	3.98	4.65	–1.84	–1.84
TRIPLE	\parallel	4.10	3.59	–2.15	–5.08
	\perp	3.98	4.66	–1.83	–2.02
Model		Distance O1–C (Å)		Binding energy (kJ/mol)	
MOF-5	Guest	CH ₄	CO ₂	CH ₄	CO ₂
<i>(b) At the MOF-5 corner</i>					
SINGLE	\parallel	4.92	5.03	–3.18	–4.94
	\perp	4.90	5.06	–3.64	–6.72
DOUBLE	\parallel	4.90	5.01	–3.11	–3.55
	\perp	4.91	5.04	–3.74	–8.14
TRIPLE	\parallel	4.92	5.04	–3.00	–2.25
	\perp	4.90	5.03	–3.80	–9.27

corner of $(\text{Zn}_4\text{O})(\text{CO}_2)_6$ and three edges of $((\text{Zn}_4\text{O})(\text{CO}_2)_6(\text{C}_6\text{H}_4))_3$ unit in perpendicular. The optimal binding sites for the CH_4 and CO_2 molecules are at the corner. CH_4 was found to point one H atom backward and along the C_3 -symmetry axis of the corner of the MOF unit cell. For CO_2 , it prefers to approach the MOF corner by moving the C atom along the C_3 axis and its molecular axis is perpendicular to the C_3 axis. The optimal binding energies for CH_4 and CO_2 are -3.64 and -9.27 kJ/mol, respectively.

Acknowledgements

The authors would like to thank the Postdoctoral Fellowship granting by the Commission on Higher Education (CHE), the Thailand research fund (TRF) and the Deutsche Forschungsgemeinschaft (DFG Project 1486/1-4) for the financial support. The Computational Chemistry Unit Cell at Department of Chemistry, Faculty of Science, Chulalongkorn University and the Scientific Mathematics Advanced Research Tasks at Department of Mathematics, Faculty of Science, Khon Kaen University, are acknowledged for all computer resources and other facilities.

References

- [1] N.L. Rosi, J. Eckert, M. Eddaoudi, D.T. Vodak, J. Kim, M. O’Keeffe, O.M. Yaghi, *Science* 300 (2003) 1127.
- [2] J.L.C. Rowsell, A.R. Millward, K.S. Park, O.M. Yaghi, *J. Am. Chem. Soc.* 126 (2004) 5666.
- [3] J.L.C. Rowsell, E.C. Spencer, J. Eckert, J.A.K. Howard, O.M. Yaghi, *Science* 309 (2005) 1350.
- [4] J.L.C. Rowsell, O.M. Yaghi, *J. Am. Chem. Soc.* 128 (2006) 1304.
- [5] H. Lir, M. Eddaoudi, M. O’Keeffe, O.M. Yaghi, *Nature* 402 (1999) 276.
- [6] M. Eddaoudi, J. Kim, N. Rosi, D. Vodak, J. Wachter, M. O’Keeffe, O.M. Yaghi, *Science* 295 (2002) 469.
- [7] O.M. Yaghi, M. O’Keeffe, N.W. Ockwig, H.K. Chae, M. Eddaoudi, J. Kim, *Nature* 423 (2003) 705.
- [8] J.L.C. Rowsell, O.M. Yaghi, *Microporous Mesoporous Mater.* 73 (2004) 3.
- [9] T. Sagara, J. Klassen, E. Ganz, *J. Chem. Phys.* 121 (2004) 1254.
- [10] T. Sagara, J. Klassen, J. Ortony, E. Ganz, *J. Chem. Phys.* 123 (2005) 14701.
- [11] T.B. Lee, D. Kim, D.H. Jung, S.B. Choi, J.H. Yoon, J. Kim, K. Choi, S.-H. Choi, *Catal. Today* 120 (2007) 330.
- [12] Q. Yang, C. Zhong, *J. Phys. Chem. B (Lett.)* 109 (2005) 11862.
- [13] T. Mueller, G. Ceder, *J. Phys. Chem. B* 109 (2005) 17974.
- [14] Q. Yang, C. Zhong, *J. Phys. Chem. B* 110 (2006) 17776.
- [15] M.J. Frisch, G.W. Trucks, H.B. Schlegel, G.E. Scuseria, M.A. Robb, J.R. Cheeseman, J.A. Montgomery, T. Vreven, K.N. Kudin, J.C. Burant, J.M. Millam, S.S. Iyengar, J. Tomasi, V. Barone, B. Mennucci, M. Cossi, G. Scalmani, N. Rega, G.A. Petersson, H. Nakatsuji, M. Hada, M. Ehara, K. Toyota, R. Fukuda, J. Hasegawa, M. Ishida, T. Nakajima, Y. Honda, O. Kitao, H. Nakai, M.L. Klene, X. Li, J.E. Knox, H.P. Hratchian, J.B. Cross, V. Bakken, C. Adamo, J. Jaramillo, R. Gomperts, R.E. Stratmann, O. Yazyev, A.J. Austin, R. Cammi, C. Pomelli, J.W. Ochterski, P.Y. Ayala, K. Morokuma, G.A. Voth, P. Salvador, J.J. Dannenberg, V.G. Zakrzewski, S. Dapprich, A.D. Daniels, M.C. Strain, O. Farkas, D.K. Malick, A.D. Rabuck, K. Raghavachari, J.B. Foresman, J.V. Ortiz, Q. Cui, A.G. Baboul, S. Clifford, J. Cioslowski, B.B. Stefanov, G. Liu, A. Liashenko, P. Piskorz, I. Komaromi, R.L. Martin, D.J. Fox, T. Keith, M.A. Al-Laham, C.Y. Peng, A. Nanayakkara, M. Challacombe, P.M.W. Gill, B. Johnson, W. Chen, M.W. Wong, C. Gonzalez, J.A. Pople, *Gaussian03, Revision C.02*, Gaussian, Inc., Wallingford CT, 2004.
- [16] B.L. Huang, A.J.H. McGaughey, M. Kaviani, *Int. J. Heat Mass Transfer* 50 (2007) 393.
- [17] C.F. Braga, R.L. Longo, *J. Mol. Struct. (Theochem.)* 716 (2005) 33.

สถาบันวิทยบริการ
จุฬาลงกรณ์มหาวิทยาลัย

Part II : Presentation

Presentations

Oral Session; 11th Annual National Symposium on Computational Science and Engineering, 27-30 March 2007, Prince of Songkla University, Phuket Campus, Phuket, Thailand

Oral Session; 2nd Progress in Advanced Materials: Micro/Nano Materials and Applications, 16-18 January 2008, Kosa Hotel, Khon Kaen, Thailand

Poster Session; 33rd Congress on Science and Technology of Thailand, 18-20 October 2007. Walailak University, Nakhon Si Thammarat, Thailand.

Poster Session; 2nd Progress in Advanced Materials: Micro/Nano Materials and Applications, 16-18 January 2008, Kosa Hotel, Khon Kaen, Thailand

Poster Session; 2nd Pure and Applied Chemistry International Conference, January 30 - February 1, 2008, Sofitel Centara Grand Bangkok, Bangkok, Thailand

Publication

The Optimal Binding Sites of CH₄ and CO₂ Molecules on the Metal-Organic Framework MOF-5: ONIOM Calculations. Chemical Physics. *Accepted*

สถาบันวิทยบริการ
จุฬาลงกรณ์มหาวิทยาลัย

VITAE

NAME: Nattaya Selphusit

DATE AND PLACE OF BIRTH: 24 May 1983 in Bangkok, Thailand

ELEMENTARY SCHOOL:

1989-1995: Wat Bangnanok School, Bangkok

SECONDARY SCHOOL:

1995-2001: Prakanong Pittayalai School, Bangkok

UNIVERSITY EDUCATION:

2001-2005: B. Sc. in Chemistry, Department of Chemistry, Faculty of Science,
Rajamangala University of Technology Krungthep, Bangkok

2005-2008: M. Sc. in Petrochemistry and Polymer Science, Faculty of Science,
Chulalongkorn University, Bangkok

*** 2 Oral and 3 poster presentations in national and international conferences**

สถาบันวิทยบริการ
จุฬาลงกรณ์มหาวิทยาลัย